ISSN-1996-918X

Pak. J. Anal. Environ. Chem. Vol. 19, No. 1 (2018) 1 – 27

http://doi.org/10.21743/pjaec/2018.06.01

Review

Photocatalytic Conversion of CO_2 Using ZnO Semiconductor by Hydrothermal Method

Kayode Adesina Adegoke[1,2], Muzaffar Iqbal[3], Hitler Louis[4], Saad Ullah Jan[3], Anam Mateen[5] and Olugbenga Solomon Bello[1*]

[1]*Department of Pure and Applied Chemistry, Ladoke Akintola University of Technology, P. M. B. 4000, Ogbomoso. Oyo State, Nigeria.*

[2]*Department of Chemistry, University of Pretoria, Pretoria, 0002, South Africa.*

[3]*National Center for Nanoscience and Technology, University of Chinese Academy of Sciences Beijing 100191 China.*

[4]*Department of Pure and Applied Chemistry, University of Calabar, P. M. B 1115 Calabar, Cross River State, Nigeria.*

[5]*Department of Chemistry, University of Sargodha, Sub-Campus Bhakkar, Pakistan.*

*Corresponding Author Email: osbello06@gmail.com

Received 30 March 2017, Revised 05 March 2018, Accepted 24 May 2018

Abstract

Photocatalytic conversion of CO_2 using ZnO semiconductor is an effective, simple, economical and attractive way of combating energy problems resulting from anthropogenic emissions of CO_2 i.e. greenhouse gases to the atmosphere. This article focuses on current advances in CO_2 photoreduction by hydrothermal method. The fundamental photocatalytic CO_2 reduction system by photocatalysts especially ZnO has been explicated. The synthetic protocol of ZnO and its growth mechanism in alkaline solution is elaborated with specific illustration of defect chemistry and its influence on CO_2 reduction activity and selectivity. Conclusively, brief challenges of its current state and future prospects were also discussed.

Keywords: ZnO semiconductor, Metal oxide photocatalysts, Hydrothermal method, Nanostructures.

Introduction

Global warming has become key challenge for the world; it is mainly due to increasing of greenhouse gases level in the environment. Carbon dioxide (CO_2) is the main contributor of this fact; it is mainly from fossil fuel combustion [1]. The Organization for Economic Cooperation and Development (OECD) Environmental viewpoint to 2050 has projected universal greenhouse gas emission to increase to around 50% from 2012 to 2050, while CO_2 emissions driven by the utilization of the conventional energy would reach up to 70 % [2-5]. In addition, by 2030, fossil fuel which is the major carbon resource has been anticipated to raise 20% of energy deliver global instead of the limited yield and high cost presently, enclosed by BP Energy Outlook 2030 [5-6]. The present use of nuclear fuels and fossil in our societies has unlimited unpleasant consequences. Fossil fuel ignition is the major cause of the changing in global climate. The atmospheric temperature is balanced at an equilibrium level by getting energy and back in to the space. Without earth atmosphere, the temperature of the earth surface would be 18^{o}C. This natural "greenhouse effect" maintains the surface temperature appropriate for existence, around 15^{o}C [7]. The additional greenhouse gases are released to the atmosphere due to the fat growing industrial development. The major supplier to these alarming rates of emissions is CO_2 from the fossil fuels combustion. Researchers estimated that these emissions cause by human has resulted in to an increase in the surface temperature of earth' sup to 0.6^{o}C [8-9]. In the last centuries the concentration of atmospheric CO_2 has been varied between 200 to 300 ppm by volume [7] However, in 2001 it reached to 370

ppm, and 399.55 ppm in January 2013 [10]. To invalidate this critical trend, alleviation technologies such as carbon consumption and storage have been reported during the last era. One of the most advantageous processes for the consumption of the environmental CO_2 is the photocatalytic reduction into the value added chemicals like conventional fuel CH_4, CH_3OH, etc. This implies that photocatalytic CO_2 reduction, is of principal significance in economic assistance by using present existing industry facilities [10].

Scientists over the world have been anxious about the issue of environment and energy, due to the less energy sources as well as environmental problems created by their utilization. This has led them in looking for substitute methods to take benefit of the clean and renewable energy resources, for instance sunlight [11]. Consequently, rapid emergence of carbon dioxide emission and the hazard pose to the environment have led us to the result that it is essential to take proper approaches to stop the building up of CO_2 [11-12]. Some existing ways to combat the concentration of CO_2 in the atmosphere include removal [13] sequestration [14-15] and conversion [15-17]. The promising method is capturing CO_2 from the atmosphere and converting it into valuable additive chemical such as CH_4 and CH_3OH using solar energy [18-19]. By developing this anthropogenic carbon cycle, simultaneously resolve the problem of the energy storage and global warming. In fact, precombustion or post combustion, CO_2 capture followed by compression and geological sequestration is one of those efforts made to reduce CO_2 emissions, but is energy intensive, hence costly. Therefore, preferable way to reduce CO_2 is recycling it as fuel with energy input from abundant source [20]. Recently, photo catalysis technology to switch CO_2 into fuel has taken the great attention of numerous scientists. It simply uses visible light or ultraviolet (UV) as source for semiconductor catalysts excitation, and the photo-excited electrons reduce water and carbon dioxide on the catalyst surface and form energy-bearing materials [21-22].

However, serious attention has been focused on the chemistry of nano-materials and reported that the chemical and physical properties of inorganic materials highly dependent on the structure, particle size and morphology [22-25], control over these factors to efficiently change their properties in an attractive method is a difficult job in the field of material synthetic chemistry [26-27]. Due to tremendous technological applications such as high stability (thermal and chemical), semiconductor nanostructures have stimulated intensive interest.

Zinc oxide (ZnO) is an important semiconductor with wide band gap (3.37 eV) and large excitation binding energy of 60 meV at room temperature. It possesses a unique position among other semiconductor materials owing to its good and wide properties such as physical and chemical stability, biocompatibility and piezoelectricity. Specially, ZnO nanoparticles are considered to be biosafe, less toxic and also biocompatible which has many applications in everyday use materials such as cosmetic, sun protection creams etc. Nowadays, ZnO nanostructure films such as nanowire [28], nanosize rods [29], nanodisks [30], nanosheet [31] nanotube [32], nanocrystal [33], etc. have broad range of applications such as sensors [34], optoelectronics [35], field emitters [36], solar cells [37] and biological applications [38]. In the past few years, tremendous experimental techniques such as metal organic vapor phase epitaxy [39], filtered vacuum arc deposition [40], pulsed laser deposition [41], vapor transport deposition [42], sputtering [43], thermal evaporation [44], metal organic chemical vapor deposition [45], electro spinning [46] etc, have been tried for growing various ZnO nanosize structures. But due to the complexity of experimental process; this makes it to be very difficult to reproduce. On the other hand, it has been demonstrated in the past few years that chemical process due to its easy, inexpensive and low-temperature process demonstrates a promising potential to fabricate ZnO nanorods. Among them, the most economical and simplest method is the solution growth technique. Comparing with other technique, the solution growth technique has many advantage like low synthesis temperature and large-scale manufacture abilities. Therefore, this process has been employed for both ZnO seed layer synthesis as well as nanorods synthesis. That is why, inventing easy and simple synthesis

method for growing ZnO nanorods proved to be a serious challenge to both scientists.

In this review, ZnO semiconductors developed or grown via hydrothermal method is our focal point, even though enormous number of literature has provided general evaluations of ZnO nanostructures [47-55]. However, we have reported here for the first time the detailed concepts of photocatalytic CO_2 reduction by ZnO semiconductor by hydrothermal method.

Basic concepts of photocatalytic reduction of CO_2

Carbon (IV) oxide (CO_2), is one of a good number thermodynamically stable compounds of carbon that exist as a linear molecule. Reduction of CO_2 to useful hydrocarbon fuels through photo catalytic method require input energy to split the C=O bond, and form the bond C–H, it involves the involvement of corresponding number of protons and multiple electrons [56]. Because of its significant high chemical state (C^{4+}) of Carbon atoms in CO_2, the process can only take place with the aids of the support called reducing agents. Thus, due to its unique nature: non-toxicity, richness and effectiveness, water (H_2O) is a preferable aspirant to act as the agent of reduction (i.e. reducing agents) compared with H_2, S^{2-}, SO_3^{2-} and amines counterparts. Photocatalytic reduction of CO_2 with H_2O is an uphill reaction with a positive change in Gibbs free energy:

$CO_2 + 2H_2O \rightarrow CH_3OH + 3/2\ O_2\ (\Delta G° = 702.20\ kJ\ mol^{-1})$ and
$CO_2 + 2H_2O \rightarrow CH_4 + 2O_2 (\Delta G° = 818.30k\ Jmol^{-1})$.

Consequently, to overcome these reaction barriers, there is need to used input energy that is supplied by incident light. As shown in (Fig. 1), the electron gets excited from the low energy level (valence band VB) to high energy level (conduction band CB) leading to simultaneously generation of equal number of holes in the conduction band when a flux of photons is absorbs by semiconductor. The electron–hole pairs resulted from photo generation separated from each other and energetically travel to catalytic active sites in the surface of semiconductor where then it encountered the electron with reducing power and this convert CO_2 in the presence of H_2O to value added hydrocarbon fuels such as CH_3OH, CO and CH_4 whereas H_2O oxidation occurs due to the oxidation capability of hole [57].

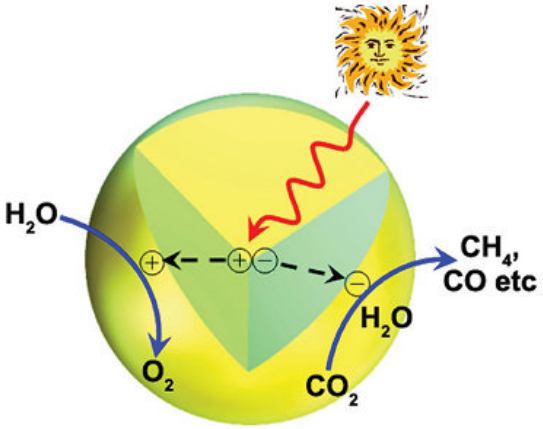

Figure 1. **Diagrammatic representation of photo induced production of an electron–hole pair in semiconductor that transfers to the outside surface for CO_2 photoredox [56]**

Nevertheless, It is important understand activation mechanism and initial carbon (IV) oxide absorption in such a way that effective photocatalyst could created to encourage absorption of CO_2. Fig. 2 gives possible configurations of adsorbed CO_2 on the photocatalyst surface [60-69].

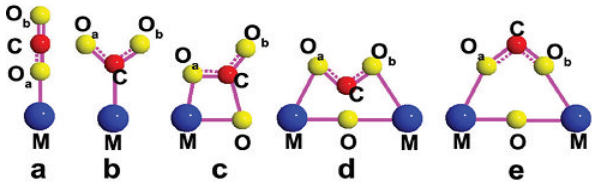

Figure 2. **Possible configurations of adsorbed CO_2 on the photocatalyst surface [60]**

The products selectivity is one of problems to be considered in the reduction of CO_2 that involves photocatalytic process, which may be affected by reaction condition, photocatalysts, including the thermodynamic reduction potentials. Figure 3 gives diverse of semiconductor photocatalysts which are relative to the redox potential of various species. Two major reasonable pathways for formation of CH_4 are proposed:

I) $CO_2 \rightarrow HCOOH \rightarrow HCHO \rightarrow CH_3OH \rightarrow CH_4$
II) $CO_2 \rightarrow CO \rightarrow C^{\bullet} \rightarrow CH_2 \rightarrow CH_4$ [70-71]

However, because of complex multi-electron transfer process involved [61,72-75], the understanding of selectivity and mechanism of photocatalysis still remain a challenges.

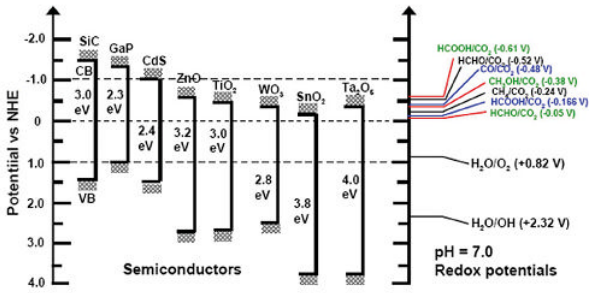

Figure 3. **Band gap energies of various semiconductor photocatalysts along with conduction band (CB), valence band (VB) potentials [70-71]**

The concept of artificial photosynthesis by metal oxide photocatalysts.

Photocatalytic CO_2 conversion utilizes semiconductors to promote reactions under the influence of light irradiation is called artificial photosynthesis. Here, our focus is only on the artificial photosynthesis by metal oxide photocatalysts. The fundamental route can be summarized into three steps:

(a) Generation of charge carriers (electron–hole pairs) upon the absorption of photons with suitable energy from light irradiation.

(b) Separation and transportation of charge carrier.

(c) Reaction of the charge carriers and surface species [76-78].

Photocatalytic conversion of CO_2 is seen to be a complicated combination of photochemical and photophysical processes. This is because the redox reaction is initiated by photo-excitation when the energy of incident photons is equal to or higher than the band gap of a semiconductor is received by a photocatalyst [79]. Then the electrons are excited from the valance band to the conduction band [80]. Fig. 4 reveals the electrons and holes undergo intra-band transitions. They have the ability to travel to the surface, combine at the trap sites (i.e. recombination process) through radiative or non-radiative pathways. Otherwise, these electrons can travel to the surface of semiconductor and react with surface adsorbed species of CO_2 if recombination happens slower than the reactions during transitions [81]. However, not all the electrons reaching the surface have the ability to reduce CO_2 which is a thermodynamically inert and very stable compound [76]. Compared with most of the reduction methods mentioned above which require high-energy input, either at high temperature and/or under high pressure [82], photosynthesis does not require extra energy except solar irradiation thus making it to have better advantages over its peers. This is because the required energy for conversion process must emerge from a process that does not release additional greenhouse gases directly into the environment. This means that other available technologies for the CO_2 conversion are not the best one contained by these criteria.

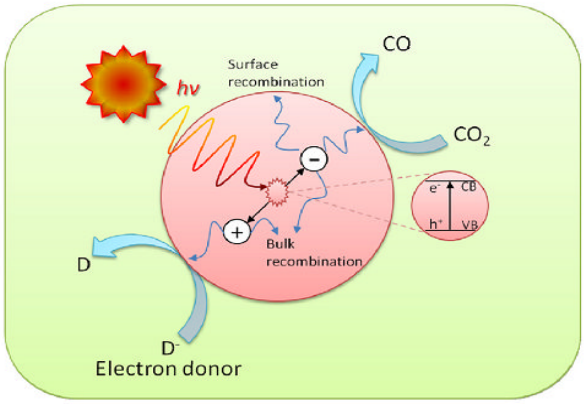

Figure 4. **Schematic diagram of photo excitation and electron transfer process [79]**

Moreover, photogenerated electrons at higher reduction potential level can offer driving force (also called over-potential) for the expected chemical reactions. This is due to the fact that reduction potential measures the capability of chemical specie to gain electrons. Species with a lower (more positive) reduction potential will gain electrons (i.e. be reduced) and those with a higher (more negative) reduction potential will lose electrons (i.e. be oxidized) [79, 83]. To facilitate the reduction of CO_2 into useful chemical (e.g. CO or hydrocarbons), it is required that electron in the

semiconductor should have more negative chemical potential as well as hole needed to be on more positive potential side for water oxidation. Therefore, (Table 1) illustrates the pathways for the production of renewable fuels especially solar and the associated potentials at pH = 7 [84].

Table 1. **Reaction mechanisms for the production of solar fuels and the associated potentials.**

Reaction	E_o (V vsNHE)	Eqn No.
$CO_2 + 2e^- \rightarrow \bullet CO_2^-$	−1.90	(1)
$CO_2 + 2H^+ + 2e^- \rightarrow HCOOH$	−0.61	(2)
$CO_2 + 2H^+ + 2e^- \rightarrow CO + H_2O$	−0.53	(3)
$CO_2 + 4H^+ + 4e^- \rightarrow HCHO + H_2O$	−0.48	(4)
$CO_2 + 6H^+ + 6e^- \rightarrow CH_3OH + H_2O$	−0.38	(5)
$CO_2 + 8H^+ + 8e^- \rightarrow CH_4 + 2H_2O$	−0.24	(6)
$2H_2O + 4h^+ \rightarrow O_2 + 4H^+$	+0.81	(7)
$2H^+ + 2e^- \rightarrow H_2$	−0.4	(8)

From a thermodynamic approach, formation of methane and methanol are more favorable in CO_2 reduction, since these reactions take place at lower potentials. However, the kinetic drawback makes methane and methanol formation more difficult and complex than carbon monoxide, formaldehyde and formic acid because more electrons are required for the former reactions [85]. In addition, the 2–8 electrons and protons reactions to obtain the desired products are extremely difficult and time consuming. As a result of the complicated nature of the inorganic photocatalyst surface, the interaction between photocatalyst and absorbed species may undergo a series of one-electron processes instead of a multi-electron, multi-proton process, thus making the actual redox potential required to be dependent on the reaction pathway. For example, if CO_2 reduction is initiated by single electron reduction of CO_2 to CO_2^-, the potential is around −1.9V vs NHE. With such concern, being able to discharge multiple electrons with protons at a time is important to improve reaction efficiency [79]. Thus, generating sufficient electron–hole pairs, separating charges efficiently and providing active catalytic sides are the paramount factors for CO_2 photoreduction.

Although, photoreduction of CO_2 shows great potential [86-87], at present one of the greatest drawbacks is the low conversion efficiency due to some associated major factors which bound the efficiency: (i) mismatching between the absorption ability of semiconductor and the solar spectrum; (ii) poor charge transfer separation efficiency; (iii) low solubility of CO_2 molecule in water (approximately 33 mol in 1 ml of water at 100 kPa and room temperature); (iv) reverse reactions during reduction of CO_2; and (v) competition reaction of water reduction to hydrogen [88]. The solar spectrum consists of 4 % of the UV radiations and 43% visible region. To find a photocatalyst which can absorb visible light, enough higher conduction band position is one of the main goals of the research that remains unresolved. Overpotential is necessary as a driving force for charge carrier transport and reactions, thus practical requirement for CO_2 conversion is usually greater than the theoretical energy required to produce the desired products [76, 89]. Even though; the direct matching the band gap of a semiconductor to the solar spectrum is challenging, hence, several strategies have been used to improve the absorption ability of an inorganic photocatalyst. Doping with elements has been a pursuit to sensitize photocatalyst with a wide band gap toward visible light absorption. As a broad and active topic, doping of photocatalysts with metal ions (Fe^{3+}, Zn^{2+}, $W^{6+,}$ etc.) and non-metal ions (C, N, S, B, etc.) have already been widely studied [90–94]. Therefore, a brief and general introduction is mentioned here. Doping does not only retard the fast charge recombination, but also introduce defect states (inter-band states or mid-gap levels) [95]. For instance, Zhang et al [96] reported that the narrowed band gap of a semiconductor after doping with non-metal ions (e.g. N or C) can be ascribed to the mixing of p-states of the dopants with O2p states to form a new valance band [96]. However, the function of doping on CO_2 conversion is still arguable and remains understudy.

Semiconductor heterostructure formation is a new effective way of enhancing the light absorption and charge separation ability of a material. Owing to band alignment, the band bending induces a built-in field, which accounts for motivating photo-excited charges to transfer in the opposite direction [97]. Semiconductor quantum dots (QDs) are also considered to be an ideal choice for the coupled component in the

heterostructures. With the existence of QDs, the visible light response of the photocatalysts can be easily adjusted. In addition, QDs can also make use of hot electrons to create multiple charge carriers when excited by a single high energetic photon thus resulting to a high amount of the charge carriers [98]. Similarly, organic dyes are often used as sensitizers to boost the visible light absorption ability of a semiconductor. Here, under irradiation, dyes can inject photo-excited electrons into the semiconductor conduction band. Hence, the electron transfer efficiency between the dye sensitizer and the semiconductor depends on many factors, which include the LUMO level of the dyes and the conduction band edge of semiconductors [99]. When CO_2 is being reduced by the photogenerated electrons, the utilization of an equal number of photogenerated holes should also be employed. Otherwise, the accumulation of the holes in a photocatalyst can probably increase the charge recombination and thereby shorten the lifetime of electrons.

Consequently, it is believed that holes could play a negative role in the photocatalytic reactions which lead to the photocorrosion of the photocatalyst and make it unstable if they were not used efficiently. This makes application of artificial electron donor to scavenge the holes a most popular solution [100]. However, the process and energy used in synthesizing the artificial electron donor must be taken into consideration since it may cause more CO_2 emission which result into more problems instead of solving the problem. Water is considered to be the ideal electron donor, nevertheless, the large water oxidation potential is the main drawback. Over the past decade, only very few photocatalysts that can reduce CO_2 and oxidize water simultaneously have been reported [101-102]. Competition from water reduction process by photogenerated electrons is a challenging area when water is used as a electron source donor.

In comparison to most of the CO_2 reduction routes, reducing water is a relative easy process in term of kinetics and thermodynamics. In thermodynamics aspect, the reduction potential of water to hydrogen is 0.0V (pH=0) which is more positive than CO_2 reduction to CO, formic acid and formaldehyde, respectively. In kinetics aspect, water reduction has a 2-electrons process which is more facile than most of the CO_2 reduction which required 4–8 electrons. While reduction of CO_2 is also limited by its low solubility in water, the water reduction does not suffer from the similar problem, thus the chance for electrons to meet and react with water is much higher than with CO_2 counterparts. Although very limited investigation has been reported to address this problem but it is generally agreed that the reaction selectivity can be controlled by modifying photocatalysts morphology, changing the exposed facets or parameters and introducing new reaction sites [103]. Thus viewed that particular atom arrangement on the surface can be more favorable to absorb CO_2 molecules than water molecule on the surface. As a result of this trend, two different morphologies of Cu_2O have been reported to have dramatic difference in products' selectivity [104]. Additionally, co-catalyst loading has also been claimed to be able to vary the reduction products' selectivity where Ag and Cu are commonly used as co-catalysts for CO_2 reduction whereas the loading of Pt or Au is more favorable for hydrogen production [79].

Synthetic methods of ZnO nanostructure for photocatalytic conversion of CO_2

Different methods have been developed to synthesize numbers of semiconductor photocatalysts. These were divided based on their preparation routes and mechanism, approaches either physical or chemical. The physical approach majorly utilizes mechanical force as an efficient means of building the solid interface in the heterostructure [105-108]. For example the pulverization of graphitic carbon nitride (g-C_3N_4) to lesser magnitude with the aid of a planetary mill to improve and make contact between g-C_3N_4 and WO_3 for preparation of the g-C_3N_4/WO_3 hybrid system has been reported to demonstrate a high catalytic activity in the CO_2 photoreduction to CH_3OH [109]. Moreover, utilization of inter-particle electrostatic force is another competent way reported to fabricate heterostructure. The HRTEM results show that g-C_3N_4 and $KNbO_3$ powder exposed the arrangement of a close contact in the g-C_3N_4/ $KNbO_3$ heterostructure. This hetero-

junction is of better quality under visible-light illumination compared to pure C_3N_4 in catalyzing the photoreduction of CO_2 to CH_4 [110].

Though the physical approach is convenient and simple way for controlling the different proportion of materials whereas the chemical approach is a more well-known approach to build the heterostructure due to the fact that the interface produced through this approach is more stable because the chemical bonding connected the materials involved. The chemical approach usually employs one material as support/substrate and another is *in-situ* grown onto its surface by means of chemical adsorption. To this point, numerous synthetic methods such as deposition–precipitation, [111] hydrothermal [112], calcinations [113-116] and electrode position, [117] were used to build a contact between the nanomaterials, physical vapor deposition metal–organic chemical vapor deposition [118–120], wet chemical technique [121–123], molecular beam epitaxy [124], sputtering [125], pulsed laser deposition [126-127], electrospinning [128-130], flux techniques [131], and also top down techniques via etching [132]. However, these techniques are costly and the selection of substrate is limited and difficult in handing.

Comparatively, among these techniques, physical vapor deposition and flux techniques generally involve an elevated temperature, and the impurities can easily be incorporate in the ZnO nanostructures. For that reason, many flexible organic substrates may seem not to be able to incorporate for future foldable and manageable electronics [133-134]. Whereas, MBE and MOCVD have ability to produce high quality ZnO nanowire array, but more often than not experience the limitation that has to do with less product yield, not uniform, and selection of substrate is limited. Moreover, the price of the experiment is commonly high, this made them to be less broadly adopted. Pulsed laser deposition, sputtering and top down techniques proved to boast of less reproducibility compared with other approaches. Electrospinning produces highly crystalline fibers. The hydrothermal method is a simplistic used method among them, with which the heterostructure can be synthesized by one-step reaction. The synthesis of ZnO semiconductors was demonstrated by a number of approaches.

Consequently, it is highly desirable to develop a simple stratagem for site-selective synthesis of nanoparticles on the ZnO nanostructure arrays while maintaining the structures for photoelectrochemical application. By comparative speaking, hydrothermal method are preferable for several reasons including low price, less dangerous, and thus capable of simple scaling up [133-134]; the growth occurs at a relatively low temperature, compatible with flexible organic substrates, no need of metal catalysts, and can be incorporated with well-developed silicon technologies [135]. Furthermore, there are different parameters that can be changed to effectively control the geometry and properties of the material [136-137]. These methods have been established as a very powerful technique for synthesizing ZnO nanostructures. For instance, Wang et al. [136] prepared facile and efficient strategy to fabricate Ag nanoparticle tip-grafted ZnO nanowire array heterostructures through the hydrothermal treatment, this produced Ag nanoparticle tip-grafted ZnO nanowire arrays (Scheme 1) both under visible-light and UV irradiation [136].

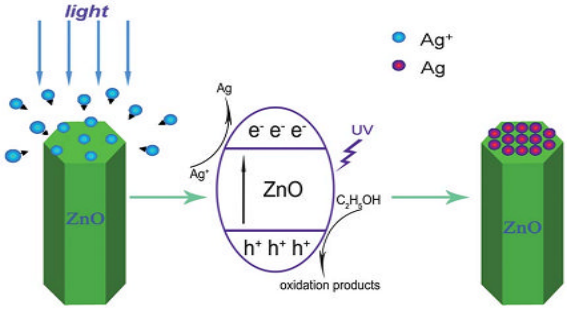

Scheme 1: **Diagrammatic representation of the photochemical reactions resulting to the formation of Ag nanoparticle tip-grafted ZnO nanowire arrays [136]**

For ZnO nanorods / nanowires, hydrothermal method has been reported as a high performance growth technique, it has recently received greater attraction due to its excellent advantages such as low price, low temperature, non-hazardous operation and environmental cordiality [138-148]. In current studies, controlled growth of well-aligned ZnO nanorods with greater optical quality was successfully achieved on glass

substrates while using hydrothermal method via optimizing the preparation parameters [113]. The growth process of ZnO nanorods was controlled by optimizing the reaction parameters, such as concentration of precursor, growth temperature and growth time. Due to its low price and ability to coat large surface areas, hydrothermal technique is reported in this review as efficient and simple method to adopt. Verges et al [122] reported the hydrothermal method of synthesizing ZnO nanostructures. But, this could not infuse much intension till when Vayssieres et al [123] successfully used the technique for the controlled synthesis of ZnO nanorods on glass and Si substrates by the thermal decomposition of methylamine and zinc nitrate. To start the growth from the substrate, a very thin layer of ZnO nanoparticles was grown on the substrate. Methenamine, also known as hexamethylen-etetramine (HMT) or hexamine is a highly water soluble, non-ionic tetradentate cyclic tertiary amine. Thermal degradation of HMT releases hydroxyl ions which react with Zn^{2+} ions to form ZnO [111]. The aqueous solutions of zinc nitrate and HMT have ability to produce the following chemical reactions.

$(CH_2)_6N_4+6H_2O \leftrightarrow 6HCHO+4NH_3$ $NH_3+H_2O \leftrightarrow NH_4^+ + OH^-$

$Zn(NO_3)_2 \bullet 6H_2O \rightarrow Zn^{2+}+2(NO_3)^-+6H_2O$ $2OH^-+ Zn^{2+} \leftrightarrow ZnO+H_2O$

The general trend is that, the role of HMT was to provide the hydroxyl ions to drive the precipitation reaction [111-113]. The concentration of HMT plays a very important role for the synthesis of ZnO nanostructure since OH^- is robustly related to the reaction that produces nanostructures. At the start, due to breakdown of zinc nitrate hexahydrate and HMT at an eminent temperature, OH^- was introduced in Zn^{2+} aqueous solution and their concentrations were enlarged. However, the separated colloidal $Zn(OH)_2$ clusters in solution would act partly as nuclei for the growth of ZnO nanorods. During the hydrothermal growth process, the $Zn(OH)_2$ solubility increases with increase in temperature. When the concentrations of Zn^{2+} and OH^- reach the critical value of the supersaturation of ZnO, ZnO nuclei formation start at the same time in the aqueous solution. Subsequently, the combination of ZnO nanoparticles causes reduction of the interfacial free energy. Due to the molecules at the surface are energetically less stable than the ones in the interior portion. So the (001) face has greater symmetry compare to other faces growing along the c-axis direction, which is the typical growth plane. Surface-to-volume ratio of the ZnO nanorod is determined by the nucleation. Then insertion of growth units into crystal lattice of the nanorods by dehydration reaction takes place. It was accomplished that the growth habit is determined by thermodynamic factor and by concentration of OH^- as the kinetic factor in aqueous solution growth. During the synthetics process of ZnO, mono Zn–OH is formed during the hydrolysis reaction and Zn–OH aggregation results in the formation of crystalline nuclei. Finally the particles in the film are oxidized and turned into oxide form during calcinations and annealing at elevated temperature thus promoting the creation of Zn–O–Zn bonds. The pre-heating at 70°C after each five times of dip coating direct to formation of high number of nuclei which favors the consequent crystal growth, along with the diffusion of Zinc species towards the nucleated grains causing grain growth and formation of nano crystalline ZnO nanorod.

Wang et al (2013) [149] reported that the uniformly distributed, vertically aligned into well-defined ZnO nanowires arrays have more surface density. Fig. 5A and B show the SEM images of the as-synthesized ZnO nanowires by a modified hydrothermal technique. Here, the cross-sectional SEM image (Fig. 5A) revealed that the as- grown ZnO nanowires have lengths and diameters range of ca. 1 μm and 100–200 nm respectively. But, when ZnO nanowire arrays were dipped into an aqueous $AgNO_3$ solution containing 20% ethyl alcohol, the graft synthesis between ZnO nanowires and Ag nanoparticles take place at once. As exposed in Fig. 5C and D, regular Ag nanoparticles have been successfully grafted on the top regions of ZnO nanowires after a 2 min illumination. Interestingly, cross-sectional SEM image clearly reveals that except for the tips of ZnO nanowires, nowhere any deposition were observed, obviously indicating that this is a site-

selective growth of Ag nanoparticles on the tips of ZnO nanowires which is achieved by this very simple and straight photo-reduction method. Many other works were also reviewed [136, 138-149].

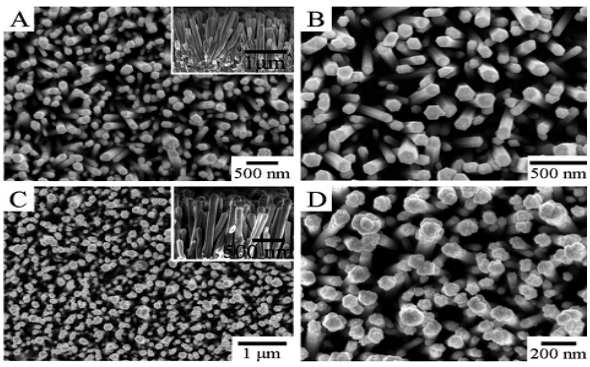

Figure 5. **Top-view SEM images of the ZnO nanowire arrays (A and B) and Ag nanoparticle tip-grafted ZnO nanowire arrays (C and D); the insets show the cross-sectional images of ZnO nanowire arrays (A) and Ag nanoparticle tip-grafted ZnO nanowire arrays (C), respectively [149]**

However, it also interesting to show comparison among difference morphology of ZnO in term of the number of active exposure surface area and dimensional. Therefore, Wang et al. focused their studies on the role of the active site for the photocatalysis. They prepared flower spindle sword and umbrella-like ZnO architecture with the hexagonal phase and investigate the photocatalytic efficiency, the result demonstrated that the flower-like ZnO possessed more irregular Zn sites than that of the spindle and sword-like ZnO with more naked Zn atoms on the defects, promoting the photoreduction reaction. Therefore relatively lower crystallinity and more defect responsible for enhanced photocatalytic activity [150]. Liu, et. al, extensively investigated ZnO nanowires for the photodegradation of organic dyes. A high photocatalytic activity and stability was ascribed to increased defects sites in ZnO nanowires. When the nanowires diameter is less than the critical value (about 50 nm) the ZnO effective band gap will increase as the redox potential there and the photogenerated charge carriers will possess higher reducing /oxidizing capabilities. The recombination of photogenerated charge carriers will be deterred with higher band gap, which will increase the catalytic performances [151].

For high photocatalytic efficiency, it is needed to have both low and high energy facets with suitable ratio in the nanostructure so as to reduce the charge recombination. The photocatalytic activity can also be enhanced by morphology modulation of other catalyst like ZnO. Different morphology of ZnO shows a significant change in stability. The Zn-terminated end has (0001) active facet in which the surface defects can enhance adsorption capability of oxygen and hydroxyl ions, resulting in increased photocatalytic efficiency. The charge separation efficiency is higher in ZnO nanorod as compared to other morphology due to its high aspect ratio. The existence of unsaturated Zinc ion in the (1010) facets is responsible for the observed high photocatalytic activity [152].

The photocatalytic CO_2 reduction activity is not only associated with the exposed facets, but also closely related to the CO_2 adsorption capability on the surface of the photocatalyst [153]. The photocatalyst with large surface area can provide more active sites and reaction centers for the photoreduction of CO_2, thus exhibiting a higher photocatalytic activity. The surface area of one dimensional ZnO nanorod is about two times larger than that of two dimensional ZnO micro flowers, which is beneficial for the photocatalytic reaction. Therefore, it is not surprising that ZnO nanorod has better photoreduction activity than other morphology. It was demonstrated that the ZnO nanorods had superior CO_2 photoreduction performance as compared to other morphology, ascribed to the synergistic effect of their large ratio of exposed (0001) facets and large surface area [153].

ZnO growth in general alkaline solutions

ZnO, an amphoteric oxide which have isoelectric point value of approximately 9.5 [154]. Mostly, ZnO is predictable to crystallize through the Zn salts hydrolysis in a basic solution which can be prepared when strong or weak alkalis are employed. Zn^{2+} is recognized to coordinate in tetrahedral complexes. Therefore, because of the electron configuration which is $3d^{10}$, it thus becomes colourless with zero crystal field

stabilization energy. Zn^{2+} though depends on the specified temperature and pH [155], have ability to exist in a sequence of intermediates, and therefore, the dehydration of intermediates can form ZnO. In aqueous media, chemical reactions are generally thought to exist in a reversible equilibrium, with the minimization of the free energy of the entire reaction system considered to be the driving force [156]. The grown of ZnO Wurtzite structure occurs along the c-axis, the energy polar surfaces such as ± (0001) (Fig 6A) which exist as O^{2-} terminated or Zn^{2+} is relatively high. Atomic arrangements along the low-index planes in hexagonal prism (Fig. 6(B)) of ZnO, $\{10\bar{1}0\}$ and $\{11\bar{2}0\}$, are stoichiometric with equal numbers of exposed Zn^{2+} or O^{2-} ions. Whereas the basal planes, (0001) and $(000\bar{1})$, and the pyramidal planes $(10\bar{1}1)$, are strongly polar and consist of sheets of Zn^{2+} or O^{2} [157]. The polar zinc-terminated surface is usually designated as (0001) and the polar oxygen-terminated surface as $(000\bar{1})$, these polar planes have high surface energy. Therefore, on forming the ZnO nucleus, the arriving precursor molecules minimize the surface energy due to its propensity to preferably adsorb on the surface that is polar. Having adsorbed the monolayer of precursor molecules, then the original polar surface would transform unto other polar surface with inverted polarity a O^{2-}-terminated surface would then change to a Zn^{2+}-terminated surface, or reverse is true. The method would then be repeated, resulting to rapid growth along the ± [0001] directions, exposing the non-polar {2110} and {1100} surfaces to the solution. This then explained 1D nanostructure fashion in solutions.

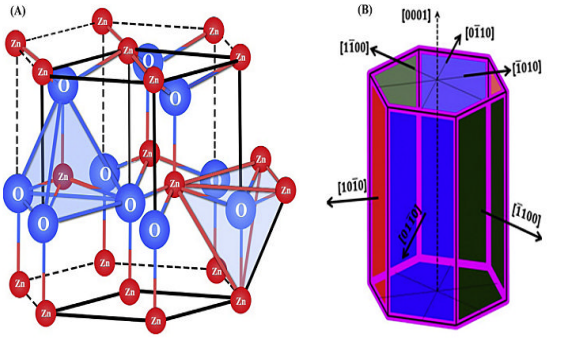

Figure 6(a). **Hexagonal wurtzite crystal structure of ZnO,** ***(b)*** **Hexagonal prism of ZnO crystal showing different crystallographic faces [158]**

An alkaline solution is necessary for the growth of ZnO nanostructures because normally divalent metal ions do not hydrolyze in acidic media [159-160] and can also be derived in a number of ways: The frequently explored alkali compounds are NaOH and KOH. In general, the ZnO solubility in an alkali solution has been reported to increase with the concentration of alkali and temperature which under a necessary condition of supersaturation, the attainment of growth zone is possible [156]. Due to a larger ion radius of K^{+}, KOH is considered to be favorable to NaOH, and thus a lower probability to incorporate into the ZnO lattice [160-163]. However, it has been revealed that OH^{-} was attracted to Na^{+} around the nanocrystal thus forming a virtual layer, which inhibits the development of nanocrystal [164].

$$Zn_2 + 2OH^{-} \rightarrow Zn(OH)_2 \quad (1)$$

$$Zn(OH)_2 + 2OH^{-} \rightarrow [Zn(OH)_4]^{2-} \quad (2)$$

$$[Zn(OH)_4]^{2-} \rightarrow ZnO_2^{2-} + 2H_2O \quad (3)$$

$$ZnO_2^{2-} + H_2O \rightarrow ZnO + 2OH^{-} \quad (4)$$

$$ZnO + OH^{-} \rightarrow ZnOOH^{-} \quad (5)$$

As shown in the Eqns 1-5, the major reactions involved in the synthesis are illustrated [165-166]. According to eqn 2, $Zn(OH)_4^{2-}$ is not necessarily the product, can also exist as $Zn(OH)_2$ or $Zn(OH)^{+}$, this thus depend on the operational parameters which include the pH value and concentration of Zn^{2+} as exposed in Fig. 7(a). These entire intermediate products were in equilibrium, and the products dominated differed under different reaction conditions. To understand this growth reaction, initially, the OH^{-} and Zn^{2+} ions coordinated with each other, underwent dehydration via proton transfer, formed $Zn^{2+}\cdots O^{2-}\cdots Zn^{2+}$ bonds, and this led to an agglomeration in the form of $[Zn_x(OH)_y]^{(2x-y)+}$, that demonstrated an octahedral geometry [60]. At the beginning, these aggregates typically contained below 50 ions, and the creation of O^{2-} ions imply an impressive change in the aggregate. This results migration of water (H_2O) molecules produced by dehydration into the solution as the reaction process proceeds. Having obtained the aggregates of such ions (about

150), the domains of wurtzite types ZnO are then nucleated in the central region of the aggregates (given away in Fig. 7(b)). The Zn^{2+} and O^{2-} ions only are the core, while the aggregate surface still principally comprises of OH^-, Zn^{2+} ions. Due to the aggregates above 200 ions exhibit by a core of nanometer sized wurtzite structure that actually grown because of additional association of OH^- and Zn^{2+} ions [162]. According to eqns (1-5), the O^{2-} in ZnO did not emerge from the solvent H_2O but from the alkali. This implies that H_2O is not necessarily requiring the solvent for the growth of ZnO [167-170]. The solvents could be organic, (e.g. butanol, methanol, ethanol) [167-169], or ionic liquids [171-172]. Under alkaline conditions, by adjusting the ratio of OH^- and Zn^{2+} the reactions can happen at room temperature, resulting ZnO nanowires even below 10 nm size. ZnO nanowires arrays with a range of aspect ratios may simply be prepared by just adjusting reaction time and OH^- concentration [168]. Several other reported works were reviewed on growth over ZnO semiconductor for enhancing photocatalytic performances [173-179].

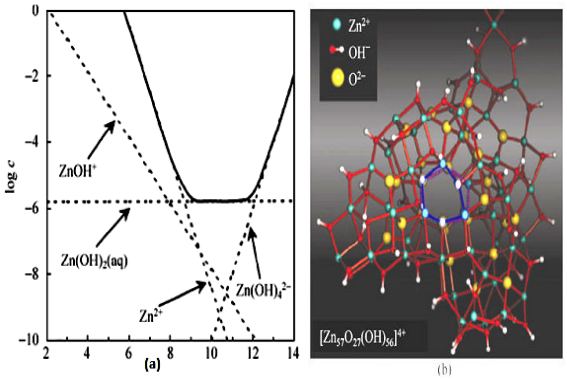

Figure 7(a). **Phase stability diagrams for the ZnO(s)–H_2O system at 25 °C as a function of precursor concentration and pH, the dashed lines indicate the thermodynamic equilibrium between the Zn^{2+} soluble species and the resultant solid phases [161].** ***(b)*** **Aggregation of domains of the wurtzite structured ZnO, where the characteristic rings in the aggregate center are highlighted in blue. The two staggered six-rings form a center of stability and give rise to further ordering in favor of the wurtzite structure [162]**

Moreover, polar inorganic nanocrystal growth is sensitive to solvents reaction, tuning and controlling their morphologies by the crystal–solvent facial interactions [167] is necessary since ZnO morphology is mainly directed by the saturated vapor pressure and polarity of the solvents [170]. As reflected in Fig. 8(a-c), the ZnO nanowires ratio is dictated by the relative growth rates of non-polar and polar surfaces and this can be changed by simply vary the polarity of the solvents. Polar solvent have been demonstrated to have strong interactions with the ZnO polar surfaces, and thereby obstructing adsorption of the precursor molecule. While going from the more polar solvent methanol to the less polar solvent 1-butanol; the aspect ratio of the ZnO semiconductors increases. The as-grown ZnO nanowires revealed two well-faceted basal planes along the ±c axis (Fig. 8d) [169]. Whenever the non-polar hexane solvent is used, very thin ZnO nanowires with 2 nm diameters would be prepared from precursor of a simple acetate (Fig. 9a) [174]. These thin nanowires are self-assembled to uniform nanowires aligned parallel to each other [170] which possibly grown by oriented coalescence of quantum dots (Fig. 9b). It was reported by Pacholski et al. [175-176] that performing an oriented attachment of quasi-spherical ZnO nanostructures would be a main reaction mechanism during the single crystalline nanowires synthesis [175-176]. The necks between the attached nanostuctures were later on filled and the Ostwald ripening was further employed to smoothen the nanowire surfaces [175].

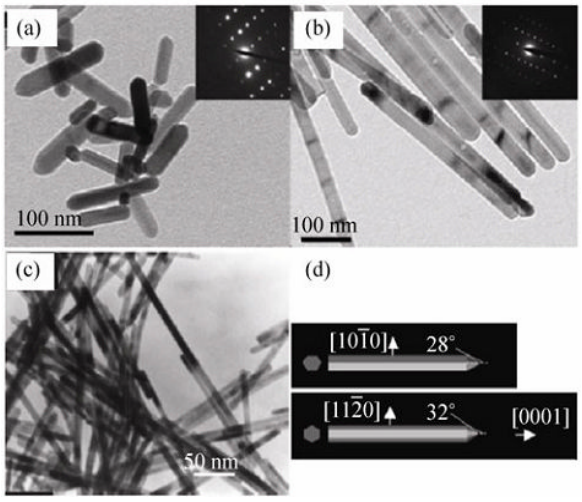

Figure 8. **TEM images of ZnO nanowires grown in solvents with different polarities: (a) methanol [167], (b) ethanol [167], and (c) 1-butanol [168]. Although the reaction temperature and the growth time are not the same, still the effect of the solvent polarity on the nanowire aspect ratio is obvious. Insets in (a) and (b) are selected area electron diffraction patterns. (d) Schematic illustration of growing +c ends of ZnO with two common interplanar angles [169]**

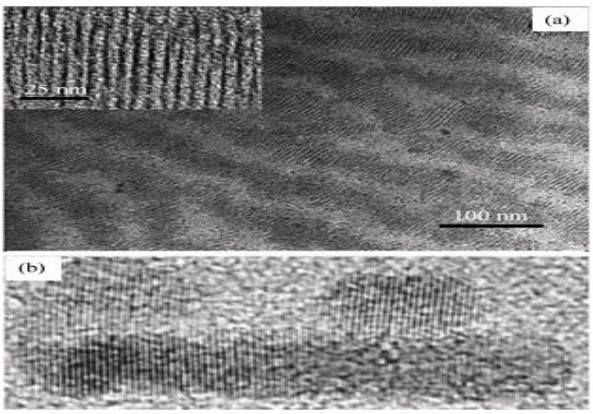

Figure 9(a). **TEM image of self-assembled ZnO nanowires with diameters of about 2 nm (inset is a higher resolution image showing the oriented stacking; nanowires are dark contrast.) [174].** ***(b)*** **TEM image of the very thin nanowire grown by orientational aggregation of several quantum dots [175]**

The derived alkaline solution could also be obtained from other amine compounds, and weak bases (e. g. $NH_3{\cdot}H_2O$) [177]. For instance, the kinetics of ZnO nanowires growth in $NH_3{\cdot}H_2O$ has been well studied [178]. Besides providing a basic environment, $NH_3{\cdot}H_2O$ has been demonstrated to mediate heterogeneous nucleation of ZnO nanowires [178–181]. Various researchers have demonstrated that depletion of Zn^{2+} ions the synthesis of the ZnO nanowires can be overcome [180-187].

ZnO defect chemistry

The associated charge carriers and control of defects is of paramount significance in applications that develop the wide range of properties of doped ZnO. Although, there are numerous works on ZnO, yet the link between defect chemistry, properties and processing, have not been given detail attention. ZnO has a simple chemical formula but possesses high defect chemistry [188]. Huge reports on defect have been reported in the past 40 years in relation to ZnO properties and applications in ZnO varistors: defects significantly change grain boundary properties and also I-V characteristics, yet, there is vital need to revisit it in the context/framework of novel application with the use of nanostructure materials [189-190]. Prior to consideration of ZnO defect structure, it is essential to understand that ZnO has open structure, with a hexagonal close packed lattice. Having all octahedral sites empty. That is why; there are abundance of sites for ZnO to accommodate intrinsic defects and extrinsic dopants. The electronic energy levels of native imperfections in ZnO are illustrated in Fig. 10 with lot of intrinsic defects with different ionization energies [191-194].

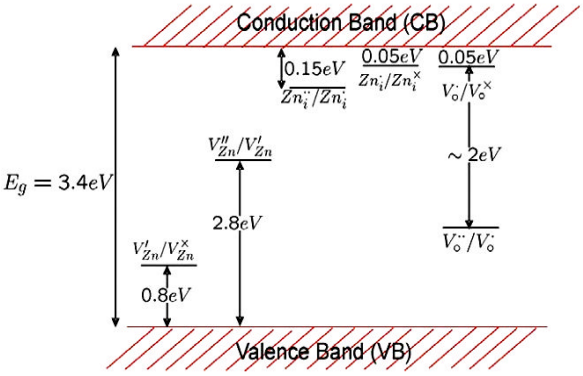

Figure 10. **Energy levels of native defects in ZnO. The donor defects $Zn_i^{\cdot\cdot}$, : $Zn_i^{\cdot}$, : $Zn_i^{\times}$, : $V_o^{\cdot\cdot}$, $V_o^{\cdot}$, V_o and the acceptor defects are: V''_{Zn}, V'_{Zn} [188], (where Zn = zinc, i = interstitial site, O = oxygen, and V = vacancy; : $Zn_i^{\cdot\cdot}$, : $Zn_i^{\cdot}$, : $Zn_i^{\times}$, : $V_o^{\cdot\cdot}$, $V_o^{\cdot}$, V_o are donor defects while V''_{Zn}, V'_{Zn} are acceptor defects respectively)**

On the other hand partial pressure of zinc, oxygen, pO_2 and pZn are also very important. So, oxygen vacancies may be predominate under high temperatures and very reducing conditions. Under Zn vapor rich environments Zn interstitials are the major defects. Even at very low temperatures like 500 °C; Zn evaporates readily, in a Zn-poor environment [193]. Annealing is required, in order to keep a Zn interstitial concentration [194]. Solubility from saturated Zn vapor is calculated to be $n = 3.4 \times 10^{20} \exp(-0.65e/kT)$ atoms/cm^3 [193]. In order to measure the defects in different pZn and pO_2 regimes, Brouwer diagrams that plot log [defect or carrier concentration] versus log pO_2 or log pZn are used. For ZnO, the Brouwer diagram is given in (Fig. 11) [194]. It shows that in the low pO_2 regime charged oxygen vacancies dominate. Still, some scientists report that in the low pO_2 regime Zn interstitials dominate [195]. This difference is likely to be a result of the influence of pZn, (at low pO_2 and high pZn). It is probable that Zn interstitials dominate, whereas at low pO_2 and low pZn and it is probable that oxygen vacancies dominate. There is wide agreement that at higher pO_2 there is a switch to Zn vacancy domination. In terms of pZn, there is a switch from Zn vacancy

domination at low pZn to Zn interstitials at higher pZn [192]. Thus, the transition occurs at around pZn ~10^{-10}atm, at 1000 °C [192]. The power dependencies of the slopes in Fig. 11 (-1/6 and ±1/2) arise from the relevant defect equilibria [196]. Across the Brouwer diagram carrier concentrations can vary by several orders of magnitude [197]. Impurities and intentional doping with differently charged ions have high effects on the defect equilibria and this is very essential to consider when nanostructure is synthesized in the existence of other atomic species. Depending on whether the ion has a lower valence (e.g. Li^{1+} introduces holes) or higher valence (e.g. Al^{3+} introduces electrons) than the Zn by keeping that in mind carriers are introduced. On the carrier concentration from such substitutions there is no pO_2 or pZn dependence, but very small atomic concentrations (>10^{16} cm^{-3}) can outweigh the intrinsic defects in the middle pO_2 or pZn regions, leading to a plateau in carrier concentration over several decades of partial pressure.

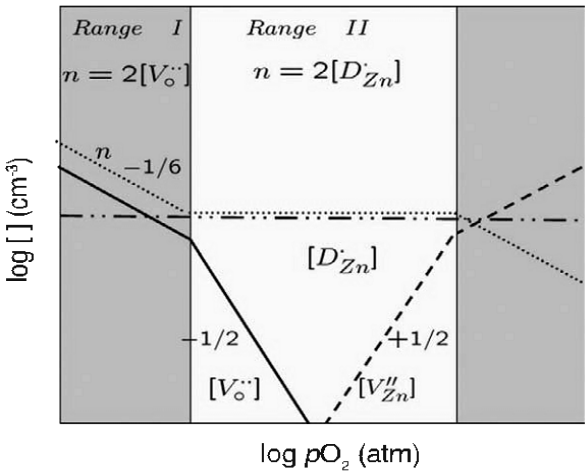

Figure 11. **Schematic Brouwer diagram showing a transition from intrinsic defect control by $V_o^{\cdot\cdot}$ (range I) to extrinsic defect control from an unknown charged donor impurity $D_{Zn}^{\cdot}$ (e.g. an ion of 3+ valence) (range II). [ ] on the left-hand axis indicates concentration of defects. The far right-hand region (unlabeled) corresponds to $V_{Zn}^{\cdot}$ control [194-197]**

In summary, Tam et. al. [198] reported that large defect concentrations in as-grown ZnO nanorods could be considerably enhanced by annealing (Fig.12) by 200 °C because of its ability to demonstrate a significant enhancement in UV to visible emission ratio, but positron annihilation measurements indicate that a significant quantity of defects are still there in the material. Photoluminescence spectra exhibition were not satisfactory results of sample defect density and quality. Sample emission intensity and defect shape are majorly reliant on the annealing temperature, and they have intricate connection between results obtained from distinct measurements. ZnO nanorods grown by hydrothermal approach shows green emission is due to the presence of surface defects and yellow emission originates from the hydroxyl groups. Due to the defect complexes show both red and green emission (involve V_{Zn}), while red emission is responsible for chemical character of defects and requires further study.

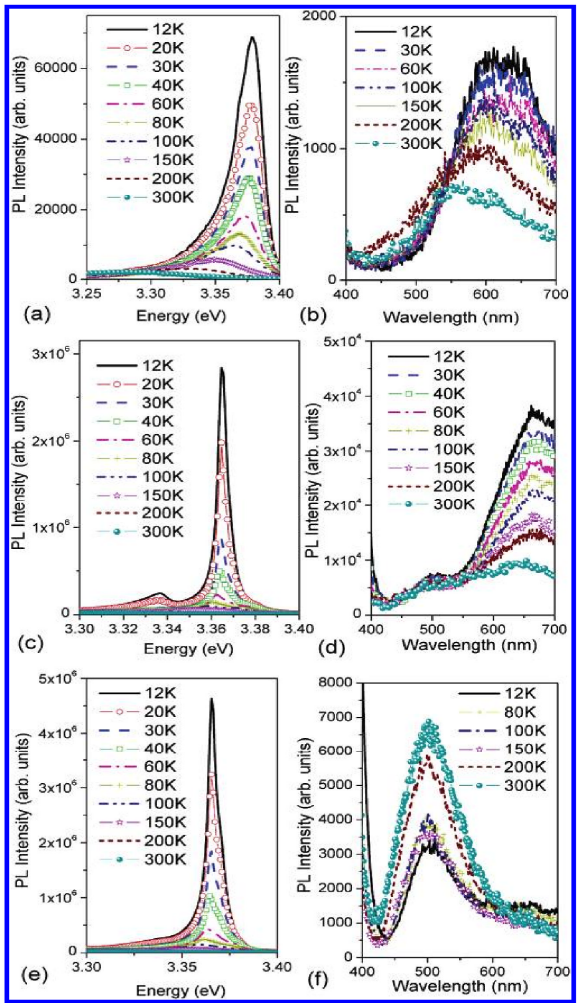

Figure 12. **Temperature dependence of the UV and defect emission for ZnO nanorods (a and b) no annealing, (c and d) annealed in air, and (e and f) annealed in forming gas [198]**

Influence of termination planes on the photocatalytic performance of ZnO

The diversity of ZnO morphologies i.e. nanowires, nanorods, core/shell, nanoflowers and nanobelts etc. are reported in literature [199-212]. The role of morphology beside balancing the light absorption depth and controlling the charge carrier diffusion length is of utmost important as it varies the type and amount of exposed crystal facets. The greater proportion of exposed facets will directly influence the photocatalytic performance. The negatively charged CO_2 reduction intermediates will more preferably bound to the terminal sites that are slightly positively charged and thus will increase the activity and selectivity of CO_2 reduction reaction. It has been reported that ZnO with exposed site [0001] has terminal Zn atom that is slightly positively charged and hence has higher photocatalytic activity for water splitting [199]. As such, it was postulated that preferential crystal growth leading to a high degree of exposure of the [0001] facets would enhance its catalytic activity. It was found that ZnO nanostructures with a higher exposure of [0001] facet exhibited stronger absorption in 400–450 nm range [199].

Particularly, for ZnO nanorods crystals a lot of efforts have been invested to change the ratio of oxygen or zinc terminated polar faces to non-polar crystal facets. In general it is claimed that higher polar to non-polar facet ratio plays significant role in photocatalytic performance [200-202]. Clearly, the knowledge of facet determined photocatalytic efficiency is mostly based on indirect evidences gleaned from ensembled average experiments. However, the photocatalytic performance is not solely dependent upon the facet abundance but also on crystal size and nature and affluence of crystal defects. Debroye et al., [203] correlated silver photo-depositions to specific structural features of the ZnO photocatalyst and revealed that ~50% of the silver nanoparticles are deposited at the outlines of structural imperfections at the nonpolar facets, 45% at the edges of the O-terminated polar facets, and the remaining 5% are distributed randomly at what appear to be defect-free locations. The latter is concluded based on the available structural resolution offered by the recorded scanning electron micrographs. This observation is remarkable because literature mostly suggests that the polar (0001) or $(000\bar{1})$ crystal facets are the most photo-catalytically active [204-208].

Moreover, hexagonal ZnO nanorods were prepared simply by hydrothermal treatment of dip-coated ZnO nanoparticles on a Si wafer with a uniform size of 4 nm (Fig. 13a) [209]. The corresponding FESEM image of Fig.14a reveals the formation of a dense array of ZnO nanorods with a uniform diameter of 100 nm and a length of 1.5 lm. Due to a one-dimensional nanostructure extended along the [0001] direction, the ZnO nanorods have a larger population of nonpolar faces than polar {0001} ones. In order to suppress crystal growth along the [0001]-axis, Jang, et al [210] tried to protect the Zn^{2+}-terminated (0001) plane, that is, Zn (0001), through complexation between Zn^{2+} ions and citrate ligands [211]. On the basis of this strategy, hexagonal nanoplates with a uniform diameter of 1.0 lm and a thickness of 50 nm were successfully obtained, as can be seen clearly from the FESEM image in Fig. 14b. Such formation of nanoplates with a high proportion of polar {0001} planes is surely due to a strong suppression of crystal growth along the [0001] axis with a relative enhancement of crystal growth along the direction, as illustrated in Fig. 13b. Similarly, the tailored synthesis of diverse ZnO nanostructures was accomplished using controlled-seeded growth of ZnO with citrate anions. The ZnO nanocolumns, consisting of the one-dimensional stacked nanoplates, were found to show enhanced photocatalytic activity towards the decomposition of 4-chlorophenol [212]. In contrast to nanocrystals, microcrystalline homologues could be prepared without nanocrystalline ZnO seeds Fig. 13c. A hydrothermal reaction of zinc acetate under basic conditions resulted in prismatic ZnO microrods, as shown in Fig.14c. Due to an increase in particle size, the area of nonpolar planes in this microrod was much reduced, compared with that of the nanorod. In addition, the morphology of the microcrystals could be further tailored by the use of acetate-intercalated zinc hydroxy

double salt (Zn-HDS) as an intermediate (Fig. 13d).

By carrying out FESEM, high-resolution transmission electron microscopy/ selected- area electron diffraction (HRTEM/SAED), and X-ray diffraction (XRD) analyses on the reaction intermediates [210], it was determined that a fraction of the outer most surface of the Zn-HDS intermediate was transformed into hexagonal ZnO crystallites under hydrothermal conditions at 95°C (the fraction depended on the pH variation of the nutrient solution), after which the surface-formed ZnO crystallites acted as nucleation centers for dumb bell-shaped ZnO microrods (hereafter referred to as DB microrods). Since the in tercalate dacetateanions in the Zn-HDS lattice were stabilized between the Zn (0001) planes through the formation of DB microrods, the Zn (0001) faces were completely masked. In fact, the FESEM image of (Fig. 14 d) revealed that the DB microrods were formed by co-sharing the acetate ligands, giving rise to the hybridization of two individual microrodcrystals. One thing to note here is that both hexagonal microrods and DB microrods turn out to have a broader size distribution than the nanorods and nanoplates [210].

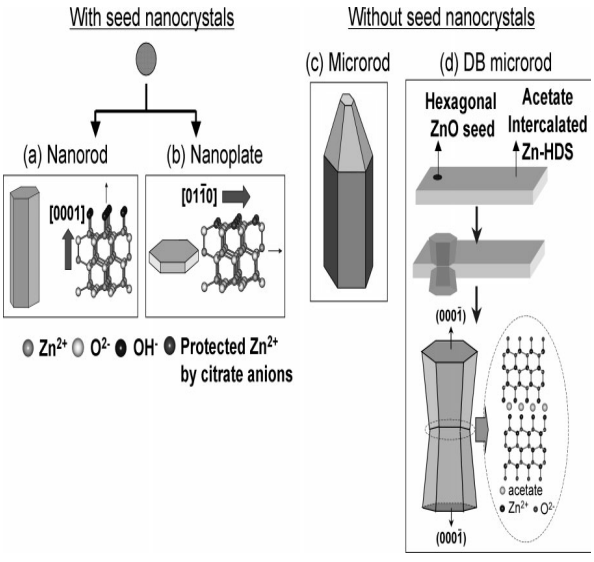

Figure 13. **Schematic illustration of the growth models for a) nanorods, b) nanoplates, c) microrods, and d) dumbell-shaped (DB) microrods of zinc oxide [210]**

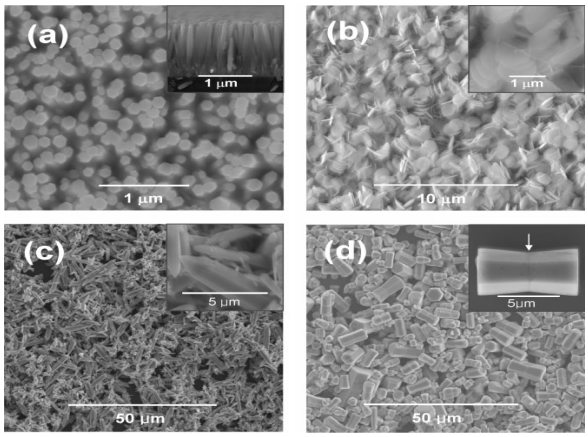

Figure 14. **FESEM images of a) nanorods, b) nanoplates, c) microrods, and d) DB microrods of zinc oxide [210]**

Influence of some parameter on the photoreduction of CO_2 over ZnO

The current advances in the photoreduction of CO_2 over semiconductor hetero-structures are reviewed in terms of charge transfer, spatial charge separation, photo-stability and visible-light activity. The first factor is the influence of visible-light activity, it should be noted here that many semiconductors wide-band gap only absorb UV light, therefore the valuable approach to improve efficiency of photo-reduction is to utilize a semiconductor with narrow-band gap to sensitize the semiconductor with wide-band gap. Numerous examples of binary sulfides [213-218], tellurides [219], selenides [218], etc have been employed couple with the semiconductors with wide-band gaps for CO_2 photoreduction. Another factor is the photo stability. In this case, the semiconductors with narrow-band gap must demonstrate an efficiency that is higher than the ones with wide-band gap as they are liable to visible light absorption. However, one major limitation here is that in practical applications, they suffer from photo-corrosion, so effort must be made to prevent this by using stable material like p-type GaP, to protect it.

Charge separation and transfer is also one of the determinant factors in photocatalytic conversion of CO_2 because semiconductor heterostructures have ability to promote the migration and separation of photogenerated charge carriers in order to lessen the electron–hole pairs

recombination thus leading to a prolonged lifetime and an improved photocatalytic activity. Many system have been designed such as p–n junction, non-p–n type II heterostructure, Z-scheme and co-catalyst,. Lastly, the hetero-phase junction, solid-state solution and hetero-facet junction must not be ignored. For more and detail understanding of these factors, readers are encouraged to go through the previous work reported [103].

Moreover, it is difficult to compare the activities of different photocatalysts reported by different groups by only considering the conversion rate or quantum efficiency due to the differences among preparation methods and in particular test conditions. However, it is agreed generally that more than a few aspects needed to be considered to advance the photocatalytic performance of semiconductors. The particle size of photocatalysts has profound consequence on the efficiency of CO_2 photoreduction [19]. Decreasing particle size can often results in the larger surface area of the photocatalysts, which serves as more active reaction sites for CO_2 adsorption. The photocatalysts with smaller particle size also benefit from the shorter transfer pathway for charge carriers to reach its surface. However, the smaller the particle size is, the more the particles' boundary, which may influence the communication between these particles and thus leads to a lower activity [19].

Furthermore, loading co-catalysts on the surface of photocatalysts is another commonly used procedure to achieve substantial enhancement on both conversion efficiency and products'selectivity. It is generally known that the photoreduction reaction can be improved by loading noble metal nanoparticles. On the other hand, metal oxide nanoparticles are found to favor the oxidation reaction. The choice of co-catalyst is crucial. Some noble metals are particular active toward water reduction while some are more suitable for CO_2 reduction. This is due to the co-catalysts providing active catalytic sites for reduction of different absorbed species [19]. The co-catalysts also extract the photogenerated electrons or holes to prolong the lifetime of the charge carriers. Although metal oxide does not provide reduction catalytic reaction side, loading it on photocatalyst may still increase the reduction products'yield, since it will extract hole and extend the lifetime of electrons for reduction reaction. In addition, electron accumulation on co-catalyst allows the discharge of more than one electron at a time, facilitating the multi-electron CO_2 reduction processes. The choice of the co-catalysts varies from different photocatalysts for reaching their best photoactivity. Thus far, the co-catalyst application strategy for CO_2 reduction is mainly focused on CO_2 reduction co-catalysts. However, there are other strategies used in photocatalytic or photoelectron catalytic (PEC) water splitting system, such as (1) oxidation co-catalysts for hole removal from photocatalyst and (2) binary co-catalysts system for both reduction and oxidation reactions [19].

Current challenges and future prospect

The main cause of global warming is the CO_2 emissions — the rate at which this is increasing recently posed a serious concerned globally; the recorded increase in 2011 was 3%. China's contribute to increase by 9% to 7.2 tonnes CO_2 average per capita CO_2 emissions, In 2011. By considering the uncertainty margin (10%) which is similar to the European Union of 7.5 tonnes per capita emissions in 2011. China is now well within the 6 to 19 tonnes/person range spanned by the major industrialized countries.

The impacts of climate change are already being observed in big as well as small cities, from severe droughts and floods to storms damaging infrastructure, worsening smog, intensified heat waves etc. Due to rate at which urbanization is increasing all over the globe, along with fast and high production of energy- and carbon-intensive building materials to build urban infrastructure [220-222]. Nearly 80 million Chinese, 20 million in the U.S and 30 million in India city dwellers live in coastal zones at risk for sea-level rise [223-225].

According to one report in 2014, China's urban population, 742 millionis contributing 10% of total world population [226]. In 2007 the countries name list with largest emitter of energy-related CO_2, China was on the top the list [227-228]. Extraordinary economic growth caused by

rapid urbanization along with the huge energy consumption and great emissions of CO_2. In 2010, Urban residents in China on average were known for causing CO_2 energy-related emissions of approximately 7 tons CO_2 emissions per capita tCO_2/capita [229]. Wuhan, rising city increases from 9.7 tCO_2/capita to 15.2 tCO_2/capita between 2005 and 2011, while emissions in Shanghai remained stable as compared to other cities, grown slightly from 12.4 tCO_2/capita to 13.1 tCO_2/capita between 2005 and 2011 [230]. In 2013, emissions London were 5.7 tCO_2/capita and 8.3 tCO_2/capita in Los Angeles [231].

China is a heavy CO_2 emitter to the atmosphere, to about 2/3 from point sources. The most straight forward way of reducing CO_2 emission consists in replacing coal fired electricity generation by renewable energy, in particular solar (China has one of the highest solar irradiances, on par with US) and wind. Besides this, recycling CO_2 using renewable energy sources offers an ideal way of reducing its climatic consequences. Liquid fuels from recycled CO_2 allow for a sustainable way of maintaining the mobility of our society, and they are easy to transport over large distances using existing infrastructure, *i.e.* pipelines, trucks and ships [232]. It can also be admixed in high fractions to gasoline and used in combustion engines. Alternatively, hydrogen can be produced on-board of automobiles via photo-reforming of methanol for use in hydrogen fuel cells [233-234], or it can be converted in a straight forward way to dimethylether or to gasoline under doubling of its energy density. Large efforts worldwide indicate the urgent nature of this substantial challenge, as evidenced by the large number of recent reviews [232-241]. These efforts included also detailed quantum-chemical calculations for both, thermal heterogeneous and photo catalysis [242-243]. Nevertheless, the subject is still awaiting a real breakthrough, in particular as regards selectivity to the desired liquid fuel product and its yield. Various products are formed, from H_2, CO, CH_4, formate and in smaller amounts methanol, ethane and other hydrocarbons, depending on the choice of the photocatalysts [232]. Therefore, research should be extended to the identification these steps by advanced spectroscopy. In addition, in practical systems, the free energy is influenced by various additional parameters, i.e. the environment (electrolyte/membrane material, potential, pressure, temperature, concentration of species, contaminations). These parameters can be influenced by the design and operation of the reactor, *e.g.* membrane reactors, micro-channel reactors, *etc*. The measurement, modeling and assessment of the effect of these parameters are to be focused through a detailed mechanistic understanding of the catalytic reduction of CO_2 into liquid fuels.

Monitoring of spectroscopic techniques using photoluminescence, EXAFS, FTIR, ESR, XANES, diffuse reflectance UV–visible, and NMR, and GC–MS to monitor isotope, electron microscopy to verify events of photocatalytic and the carbon source used for producing the fuels. The mechanism of reaction behind photo catalysis is still far from understanding especially methane formation from $CO_2 + H_2O$ when ZnO is used need to explain more clearly. Though, there are progresses on the theoretical approach which based on the band energy and the redox potential comparison but this not enough to explain the product selectivity especially when ZnO is being employed. Moreso, efficiency for the CO_2 conversion are highly expected to be further improved by combining different photocatalysts and the utilization of novel reaction systems e.g. sacrificial electron donors need to be recycled and CO_2 photoconversion to fuels should utilize anode oxidation and cathode reduction compartments. In particular, the combination of water photo-splitting to produce H_2 (or protons and electrons) and photoreduction of CO_2 with the produced H_2 have the potential of boosting the CO_2 conversion efficiency.

In addition, despite an encouraging progress achieved toward conversion of CO_2using sunlight, additional attempt is still necessary to increase photo-conversion efficiency of sunlight-to-fuel. Urgent research opportunities include uniform co-catalyst sensitization of the entire surface of ZnO nanorod for enhancing the rates of conversion. The co-catalysts design must be improved and the product selectivity needs to be controlled. Highly efficient photocatalytic materials will enable the utilization of flow

through photo catalytic membranes, in which water vapor and CO_2 can enter one side of the nanorod array membrane with a fuel exiting from the other.

Conclusion

The conversion of CO_2 into value added products is still a challenging task that demands a keen attention of researchers. To simulate the further research on unresolved issues that deserve experimental attention, it is particularly interesting to study the mechanistic aspects of photocatalytic CO_2 reduction using hydrothermal method for energy storage over ZnO semiconductor with well-defined structure and stability. It is observed that all these existing methods and techniques involve some chemicals that are environment unfriendly and hazardous. However, there are no reports available that effectively explain the redox mechanism of CO_2 reduction reaction on ZnO-based photocatalysts. Here we presented that the visible photocatalytic activity, electron-hole separation, photostability, electrode-electrolyte charge transfer and morphological influence in photocatalytic CO_2 reduction system. This article enables the investigations of system design, the choice of catalyst and morphology to facilitate the CO_2 reduction and also simulate further research in the field of photocatalysis. We also established clearly here that ZnO semiconductors have a higher population of polar Zn (0001) faces with ability to enhance the photocatalytic activity of CO_2 conversion via hydrothermal method. Moreover, the tuning of the face orientation have ability produce an optimised photocatalytic conversion of CO_2 to liquid fuels using ZnO semiconductor by hydrothermal method. Successful morphology tuning is also of great important in obtaining high polar to non-polar facets ratios so as to increase the percentage of reactive sites. Controlling the shape, size, and preferred ZnO semiconductors orientation to tailor their chemical and physical properties for optimal reactivity and selectivity are very essential.

Acknowledgements

Authors acknowledge the support obtained from The World Academy of Science (TWAS) in form of Research grants; Research Grant number: 11-249 RG/CHE/AF/AC_1_UNESCO FR: 3240262674 (2012), 15-181 RG/CHE/AF/AC_1_: 3240287083 (2015), 2016 TETFund Institution Based Research Intervention and NRF-TWAS for Doctoral Fellowship programme awarded to the first author (UID:105453 & Reference: SFH160618172220) respectively. All figures cited in this review are reproduced with permission from respective publishers.

References

1. C. M. White, B. R. Strazisar, E. J. Granite, J. S. Hoffman and H. W. Pennline, *J. Air Waste Manage. Assoc.* 53 (2003) 645. https://doi.org/10.1080/10473289.2003.10466620
2. OECD Environmental Outlook to 2050: The Consequences of Inaction, OECD, (2012) 22. http://dx.doi.org/10.1787/9789264122246-en
3. Y. Izumi, *Coord. Chem. Rev*., 257 (2013) 171. https://doi.org/10.1016/j.ccr.2012.04.018
4. N. Ahmed, Y. Shibata, T. Taniguchi and Y. Izum, *J. Catal*. 279 (2011) 123. https://doi.org/10.1016/j.jcat.2011.01.004
5. I. A. Shkrob, T. W. Marin, H. He and P. Zapol, *J. Phys. Chem.*, (2012) 116, 9450 https://doi.org/10.1021/jp300122v
6. BP Energy Outlook 2030, BP, London, (2013) 21. https://www.bp.com/content/dam/bp/en/corporate/pdf/energy-economics/energy-outlook/bp-energy-outlook-2013.pdf
7. M. Tahir and N. S. Amin, *Renew. Sust. Energ. Rev.*, 25 (2013) 560. https://doi.org/10.1016/j.rser.2013.05.027
8. B. Godfrey, Renewable Energy Power for a Sustainable Future. Oxford, UK: Oxford University Press, (2004). ISBN0199545332, 9780199545339
9. Intergovernmental Panel on Climate Change. (2001). http://streitcouncil.org/uploads/PDF/Report-Climate%20Change%202007-%20Impacts,%20Adaptation,%20and%20Vulnerability.pdf
10. National Oceanic and Atmospheric Administration National Climatic Data Center. https://www.ncdc.noaa.gov/cdo-web/

11. Y. S. Choi, J. W. Kang, D. K. Hwang, S. J. Park, *IEEE Trans. Electron Devices*, 57 (2010) 26. https://doi.org/10.1109/TED.2009.2033769
12. M. Mikkelsen, M. Jorgensen and F. C. Krebs *Energy Environ Sci.*, 3 (2010) 43. https://doi.org/10.1039/B912904A
13. A. C. Yeh and H. Bai, *Sci. Total Environ.*, 228 (1999) 121. https://doi.org/10.1016/S0048-9697(99)00025-X
14. L. Klaus, *Science*, 300 (2003) 1677. https://doi.org/10.1126/science.1079033
15. S. Bachu, *Energy Convers. Manage*., 41 (2000) 953. https://doi.org/10.1016/S0196-8904(99)00149-1
16. Y. He, Y. Wang, L. Zhang, B. Teng and M. Fan, *Appl. Catal. B. Environ*., 168 (2015) 1. https://doi.org/10.1016/j.apcatb.2014.12.017
17. R. K. Richter, T. Ming and S. Caillol, *Renew Sust. Energ. Rev*., 19 (2013) 82. https://doi.org/10.1016/j.rser.2012.10.026
18. L. Yuan and Y. J. Xu, *Appl. Surf. Sci*., 342 (2015) 154. https://doi.org/10.1016/j.apsusc.2015.03.050
19. X. Li, J. Q. Wen, J. X. Low, Y. P. Fang and J. G. Yu, *Sci. Chin. Mater*., 57 (2014) 70. https://doi.org/10.1007/s40843-014-0003-1
20. Y. Li, W. N. Wang, Z. Zhan, M. H. Woo, C. Y. Wu and P. Biswas, *Appl. Catal. B Environ*., 100 (2010) 386. https://doi.org/10.1016/j.apcatb.2010.08.015
21. M. Kitano, M. Matsuoka, M., Ueshima and M. Anpo, *Appl. Catal. A-Gen.*, 325 (2007)1. https://doi.org/10.1016/j.apcata.2007.03.013
22. A. Wei, L. Pan and W. Huang, *Mater. Sci. Eng.*, 176 (2011) 1409. https://doi.org/10.1016/j.mseb.2011.09.005
23. Y. C. Zhu, T. Mei, Y. Wang and Y. T. Qian, *J. Mater. Chem.*, 21 (2011) 11457. https://doi.org/10.1039/c1jm11079a
24. W. Xiao, D. L. Wang and X. W. Lou, *J. Phys. Chem.*, 114 (2010) 1694. https://doi.org/10.1021/jp909386d
25. X. Y. Li, Z. J. Si, Y. Q. Lei, X. N. Li, J. K. Tang, S. Y. Song and H. J. Zhang, *Cryst. Eng. Comm.*, 13 (2011) 642. https://doi.org/10.1039/C0CE00217H
26. H. Dong, X. J. Li, Q. Peng, X. Wang, J. P. Chen and Y. D. Li, *Angew. Chem., Int. Ed.*, 44 (2005) 2782. https://doi.org/10.1002/anie.200462551
27. Y. Li, M. H. Cao and L. J. Feng, *Langmuir*, 25 (2009) 1705. https://doi.org/10.1021/la803682d
28. J. H. Shin, J. Y. Song and H. M. Park, *Mater. Lett*., 63 (2009) 145. https://doi.org/10.1016/j.matlet.2008.09.047
29. Z. Zhang, H. Yu, Y. Wang and M.Y. Han, *Nanotechnol*., 17 (2006) 2994. https://doi.org/10.1088/0957-4484/17/12/029
30. P. X. Gao, C. S. Lao, Y. Ding and Z. L. Wang, *Adv. Funct. Mater*., 16 (2006) 53. https://doi.org/10.1002/adfm.200500301
31. S. Chen, Y. Liu, C. Shao, R. Mu, Y. Lu, J. Zhang, D. Shen and X. Fan, Adv. Mater., 17 (2005) 586. https://doi.org/10.1002/adma.200401263
32. Q. Li, V. Kumar, Y. Li, H. Zhang, T. J. Marks and R. P. H. Chang, *Chem. Mater*., 17 (2005) 1001. https://doi.org/10.1021/cm048144q
33. J. J. Cole, X. Wang, R. J. Knuesel and H. O. Jacobs, *Adv. Mater*., 20 (2008) 1474. https://doi.org/10.1002/adma.200703102
34. T. Gao and T. H. Wang, *Appl. Phys. A: Mater. Sci. Process*, 80 (2005) 7. doi: 10.1007/s00339-004-3075-2
35. X. Wang, C. J. Summers and Z. L. Wang, *Nano Lett.*, 4 (2004) 423. https://doi.org/10.1021/nl035102c
36. H. Hu, K. Yu, J. Zhu and Z. Zhu, *Appl. Surf. Sci.*, 252 (2006) 8410. https://doi.org/10.1016/j.apsusc.2005.11.060
37. J. B. Baxter, A. M. Walker, K. V. Ommering and E. Saydil, *Nanotechnol.*, 17 (2006) S304. https://doi.org/10.1088/0957-4484/17/11/S13
38. T. Y. Liu, H. C. Liao, C. C. Lin, S. H. Hu and S. Y. Chen, *Langmuir*, 22 (2006) 5804. https://doi.org/10.1021/la052363o
39. K. Kitamura, T. Yatsui, M. Ohtsu and G. C. Yi, *Nanotechnol.*, 19 (2008) 175305. https://doi.org/10.1088/0957-4484/19/17/175305
40. N. Parkansky, G. Shalev, B. Alterkop, S. Goldsmith, R. L. Boxman, Z. Barkay, L.

Glikman, H. Wulff and M. Quaas, *Surf. Coat. Technol.*, 201 (2006) 2844. https://doi.org/10.1016/j.surfcoat.2006.05.032
41. Y. W. Sun and Y. Y. Tsui, *Opti. Mater.*, 29 (2006) 1111. https://doi.org/10.1016/j.optmat.2006.05.011
42. H. Tang, L. Zhu, Z. Ye, H. He, Y. Zhang, M. Zhi, F. Yang, Z. Yang and B. Zhao, *Mater. Lett.*, 61 (2007) 1170. https://doi.org/10.1016/j.matlet.2006.06.085
43. Y. H. Hwang, S-J. Seo and B-S. Bae, *J. Mater. Res.*, 25 (2010) 695. https://doi.org/10.1557/JMR.2010.0103
44. T. Ghoshal, S. Biswas, S. Kar, A. Dev, S. Chakrabarti and S. Chaudhuri, *Nanotechnol.*, 19 (2008) 065606. https://doi.org/10.1088/0957-4484/19/6/065606
45. Y. Tak, K. Yong and C. Park, *J. Cryst. Growth*, 285 (2005) 549. https://doi.org/10.1016/j.jcrysgro.2005.09.052
46. P. Viswanathamurthi, N. Bhattarai, H. Y. Kim and D. R. Lee, *Nanotechnol.*, 15 (2004) 320. https://doi.org/10.1088/0957-4484/15/3/015
47. U. Ozgur., Y. I. Alivov., C. Liu., A. Teke., M. A. Reshchikov., S. Dogan., V. Avrutin., S. J. Cho and H. J. Morkoc, *Appl. Phys.*, 98 (2005) 041301. https://doi.org/10.1063/1.1992666
48. D. C. Look, *Mat. Sci. Eng. B. Adv.*, 80 (2001) 383. https://doi.org/10.1016/S0921-5107(00)00604 -8
49. Y. W. Heo, D. P. Norton, L. C. Tien, Y. Kwon, B. S. Kang, F. Ren, S. J. Pearton and J. R. LaRoche, *Mat. Sci. Eng. R.*, 47 (2004)1. https://doi.org/10.1016/j.mser.2004.09.001
50. G. C. Yi., C. R. Wang and W. I. Park, *Semicond. Sci. Technol.*, 20 (2005) S22. https://doi.org/10.1088/0268-1242/20/4/003
51. Z. L. Wang, J. Nanosci. *Nanotechnol.*, 8 (2008) 27. https://doi.org/10.1166/jnn.2008.N08
52. N. Kamarulzaman, M. F. Kasim and R. Rusdi, *Nanoscale Res. Lett.*, 10 (2015) 346. https://doi.org/10.1186/s11671-015-1034-9
53. S. J. Pearton, D. P. Norton., K. Ip., Y. W. Heo and T. Steiner, *Prog. Mater. Sci.*, 50 (2005) 293. https://doi.org/10.1016/j.pmatsci.2004.04.001
54. C. Klingshirn, *Phys. Status Solidi B*, 244 (2007) 3027. https://doi.org/10.1002/pssb.200743072
55. L. Schmidt-Mende and J. L. MacManus, *Driscoll, Mater. Today*, 40 (2007) 10. https://doi.org/10.1016/S1369-7021(07)70078-0
56. D. G. Nocera, *Acc. Chem. Res.*, 45 (2012) 767 . https://doi.org/10.1021/ar2003013
57. A. L. Linsebigler, G. Q. Lu and J. T. Yates, *Chem. Rev.*, 95 (1995) 735. https://doi.org/10.1021/cr00035a013
58. A. J. Morris, G. J. Meyer and E. Fujita, *Acc. Chem. Res.*, 42 (2009) 1983. https://doi.org/10.1021/ar9001679
59. K. Tanaka and D. Ooyama, *Coord. Chem. Rev.*, 226 (2002) 211. https://doi.org/10.1016/S0010-8545(01)00434-9
60. L. Liu, W. L. Fan, X. Zhao, H. G. Sun, P. Li and L. M. Sun, Langmuir, 28 (2012) 10415. https://doi.org/10.1021/la301679h
61. V. P. Indrakanti, J. D. Kubicki and H. H. Schobert, *Energy Environ. Sci.*, 2 (2009) 745. https://doi.org/10.1039/b822176f
62. S. Xie, Y. Wang, Q. Zhang, W. Fan, W. Deng and Y. Wang, *Chem. Commun.*, 49 (2013) 2451. https://doi.org/10.1039/c3cc00107e
63. N. M. Dimitrijevic, B. K. Vijayan, O. G. Poluektov, T. Rajh, K. A. Gray, H. Y. He and P. Zapol, *J. Am. Chem. Soc.*, 133 (2011) 3964. https://doi.org/10.1021/ja108791u
64. J. Lee, D. C. Sorescu and X. Y. Deng, J. Am. Chem. Soc., 133 (2011) 10066. https://doi.org/10.1021/ja204077e
65. S. J. Tan, Y. Zhao, J. Zhao, Z. Wang, C. X. Ma, A. D. Zhao, B. Wang, Y. Luo, J. L. Yang and J. G. Hou, *Phys. Rev.*, (2011) 84. https://doi.org/10.1103/PhysRevB.84.155418
66. W. H. Koppenol and J. D. Rush, J. Phys. Chem., 91 (1987) 4429. https://doi.org/10.1021/j100300a045
67. V. P. Indrakanti, H. H. Schobert and J. D. Kubicki, Energy Fuels, 23 (2009) 5247. https://doi.org/10.1021/ef9003957

68. H. J. Freund and M. W. Roberts, *Surf. Sci. Rep.*, 25 (1996) 225. https://doi.org/10.1016/S0167-5729(96)00007-6
69. C. J. Gagliardi, B. C. Westlake, C. A. Kent, J. J. Paul, J. M. Papanikolas and T. J. Meyer, *Coord. Chem. Rev.*, 254 (2010) 2459. https://doi.org/10.1016/j.ccr.2010.03.001
70. A. Dhakshinamoorthy, S. Navalon, A. Corma and H. Garcia, *Energy Environ. Sci.*, 5 (2012) 9217. https://doi.org/10.1039/c2ee21948d
71. G. H. Liu, N. Hoivik, K. Y. Wang and H. Jakobsen, *Sol. Energy Mater. Sol. Cells*, 105 (2012) 53. https://doi.org/10.1016/j.solmat.2012.05.037
72. G. R. Dey, J. Nat. Gas Chem., 16 (2007) 217. https://doi.org/10.1016/S1003-9953(07)60052-8
73. K. Koci, L. Obalova and Z. Lacny, *Chem. Pap.*, 62 (2008) 1. doi: 10.2478/s11696-007-0072-x
74. S. C. Roy, O. K. Varghese, M. Paulose and C. A. Grimes, *ACS Nano*, 4 (2010) 1259. https://doi.org/10.1021/nn9015423
75. M. R. Hoffmann, J. A. Moss and M. M. Baum, Dalton Trans., 40 (2011) 5151. https://doi.org/10.1039/c0dt01777a
76. Peng Zhang, Tuo Wang, Xiaoxia Chang and Jinlong *Gong Acc. Chem. Res.*, 49 (2016) 911. https://doi.org/10.1021/acs.accounts.6b00036
77. X. Chen, S. Shen, L. Guo and S. Mao, *Chem. Rev.*, 110 (2010) 6503. https://doi.org/10.1021/cr1001645
78. H. Chen, C. Nanayakkara and V. Grassian, *Chem. Rev.*, 112 (2012) 5919. https://doi.org/10.1021/cr3002092
79. K. Li, X. An, K. H. Park, M. Khraisheh and J. Tang, *Catal. Today*, 224 (2014)3. https://doi.org/10.1016/j.cattod.2013.12.006
80. W. Fan, Q. Zhang and Y. Wang, *Phys. Chem. Chem. Phys.*, 15 (2013) 2632. https://doi.org/10.1039/c2cp43524a
81. P. Kamat, *J. Phys. Chem. Lett.*, 3 (2012) 663. https://doi.org/10.1021/jz201629p
82. P. Usubharatana, D. McMartin, A. Veawab and P. Tontiwachwuthikul, *Ind. Eng. Chem. Res.*, 45 (2006) 2558. https://doi.org/10.1021/ie0505763
83. Z. Li, W. Luo, M. Zhang, J. Feng and Z. Zou, *Energy Environ. Sci.*, 6 (2013) 347. https://doi.org/10.1039/C2EE22618A
84. A. Kubacka, M. Fernandez-García and G. Colon, *Chem. Rev.*, 112 (2012) 1555. https://doi.org/10.1021/cr100454n
85. S. Navaln, A. Dhakshinamoorthy, M. Alvaro and H. Garcia, *Chem. Sus. Chem.*, 6 (2013) 562. https://doi.org/10.1002/cssc.201200670
86. H. Zhou, J. Guo, P. Li, T. Fan and D. Zhang, *J. Ye, Sci. Rep.*, 3 (2013) 1. http://www.nature.com/srep/2013/130416/srep01667/full/srep01667.html?WT.mc_id=FBK_SciReports
87. X. Zhang, F. Han, B. Shi, S. Farsinezhad, G. P. Dechaine and K. Shankar, Angew. *Chem. Int. Ed.*, 51 (2012) 12732. https://doi.org/10.1002/anie.201205619
88. Y. Izumi, Coord. *Chem. Rev.*, 257 (2013) 171. https://doi.org/10.1016/j.ccr.2012.04.018
89. P. Liao and E. Carter, *Chem. Soc. Rev.*, 42 (2013) 2401. https://doi.org/10.1039/C2CS35267B
90. M. Dozzi and E. Selli, J. Photochem. *Photobiol. C*, 14 (2013) 13. https://doi.org/10.1016/j.jphotochemrev.2012.09.002
91. M. Pelaez, N. Nolan, S. Pillai, M. Seery, P. Falaras, A. Kontos, P. Dunlop, J. Hamilton, J. Byrne, K. O'Shea, M. Entezari and D. Dionysiou, *Appl. Catal. B-Environ.*, 125 (2012) 331. https://doi.org/10.1016/j.apcatb.2012.05.036
92. R. Daghrir, P. Drogui and D. Robert, *Ind. Eng. Chem. Res.*, 52 (2013) 3581. https://doi.org/10.1021/ie303468t
93. S. Kumar and L. Devi, *J. Phys. Chem. A*, 115 (2011) 13211. https://doi.org/10.1021/jp204364a
94. M. Rauf, M. Meetani and S. Hisaindee, *Desalination*, 276 (2011) 13. https://doi.org/10.1016/j.desal.2011.03.071
95. H. Parka, Y. Parkb, W. Kimb and W. Choib, J. Photochem. *Photobiol. C*, 15 (2013) 1.

https://doi.org/10.1016/j.jphotochemrev.2012.10.001
96. H. Zhang, G. Chen and D. Bahnemann, *J. Mater. Chem.*, 19 (2009) 5089. https://doi.org/10.1039/b821991e
97. Y. Wang, Q. Wang, X. Zhan, F. Wang and S. Muhammad, *J. He, Nanoscale*, (2013) http://dx.doi.org/10.1039/C3NR01577G.
98. R. Selinsky, Q. Ding, M. Faber, *J. Wrightand S. Jin, Chem. Soc. Rev.*, 42 (2013) 2963. https://doi.org/10.1039/C2CS35374A
99. C. Windle, R. Perutz, *Coord. Chem. Rev.*, 256 (2012) 2562. https://doi.org/10.1016/j.ccr.2012.03.010
100. A. D. Handoko, K. Li and J. Tang, *Curr. Opin. Chem. Eng.*, 2 (2013) 200. https://doi.org/10.1016/j.coche.2012.12.003
101. J. Tang, J. Durrant and D. Klug, *J. Am. Chem. Soc.*, 130 (2008) 13885. https://doi.org/10.1021/ja8034637
102. J. Tang, A. J. Cowan, J. R. Durrant and D. R. Klug, *J. Phys. Chem. C*, 115 (2011) 3143. https://doi.org/10.1021/jp1080093
103. N. Y. Wang, S. C. Yan and Z. G. Zou, *Curr. Org. Chem.*, 17 (2013) 2454. https://doi.org/10.2174/13852728113179990059
104. A. D. Handoko and J. Tang, *Int. J. Hydrogen Energy*, 38 (2013) 13017. https://doi.org/10.1016/j.ijhydene.2013.03.128
105. Z. W. Pan, Z. R. Dai and Z. L. Wang, *Science*, 291 (2001) 1947. https://doi.org/10.1126/science.1058120
106. M. H. Huang, Y. Y. Wu, H. Feick, N. Tran, E. Weber and P. D. Yang, Adv. Mater., 13 (2001) 113. https://doi.org/10.1002/1521-4095(200101)13:2<113::AID-ADMA113>3.0.CO;2-H
107. B. D. Yao, Y. F. Chan and N. Wang, *Appl. Phys. Lett.*, 81 (2002) 757. https://doi.org/10.1063/1.1495878
108. Y. Bessekhouad, D. Robert and J. V. Weber, *J. Photochem. Photo. Biol., A*, 163 (2004) 569. https://doi.org/10.1016/j.jphotochem.2004.02.006
109. T. Ohno, N. Murakami, T. Koyanagi and Y. Yang, *J. CO2 Util.* 6 (2014) 17. https://doi.org/10.1016/j.jcou.2014.02.002
110. H. Shi, C. Zhang, C. Zhou and G. Chena, *RSC Adv.*, 5 (2015) 93615. https://doi.org/10.1039/C5RA16870H
111. M. Abou Asi, C. He, M. Su, D. Xia, L. Lin, H. Deng, Y. Xiong, R. Qiu and X.-z. Li, *Catal. Today*, 175 (2011) 256. https://doi.org/10.1016/j.cattod.2011.02.055
112. X. Li, J. Chen, H. Li, J. Li, Y. Xu, Y. Liu and J. Zhou, J. Nat. *Gas Chem.*, 20 (2011) 413. https://doi.org/10.1016/S1003-9953(10)60212-5
113. J. Fu, S. Cao and J. Yu, *J. Materiomics*, 1 (2015) 124. https://doi.org/10.1016/j.jmat.2015.02.002
114. S. Zhou, Y. Liu, J. Li, Y. Wang, G. Jiang, Z. Zhao, D. Wang, A. Duan, J. Liu and Y. Wei, *Appl. Catal. B*, 20 (2014) 158. https://doi.org/10.1016/j.apcatb.2014.03.037
115. N. Zhang, S. Ouyang, T. Kako and J. Ye, *Chem. Commun.*, 48 (2012) 1269. https://doi.org/10.1039/C2CC16900B
116. C. Wang, R. L. Thompson, P. Ohodnicki, J. Baltrus and C. Matranga, *J. Mater. Chem.*, 21 (2011) 13452. https://doi.org/10.1039/c1jm12367j
117. J. Wang, G. Ji, Y. Liu, M. A. Gondal and X. Chang, *Catal. Commun.*, 46 (2014) 17. *https://doi.org/10.1016/j.catcom.2013.11.011*
118. W. I. Park., G. C. Yi., M. Y. Kim and S. Pennycook, *J. Adv. Mater.*, 14 (2002) 1841. https://doi.org/10.1002/adma.200290015
119. W. I. Park., D. H. Kim., S. W. Jung. and G. C. Yi, *Appl. Phys. Lett.*, 80 (2002) 4232. https://doi.org/10.1063/1.1482800
120. H. Yuan, Y. J. Zhang, *Cryst. Growth*, 263 (2004) 119. https://doi.org/10.1016/j.jcrysgro.2003.11.084
121. R. A. Laudise and A. A. Ballman, *J. Phys. Chem.*, 64 (1960) 688. https://doi.org/10.1021/j100834a511
122. M. A. Verges., A. Mifsud. and C. J. J. Serna *Chem. Soc. Faraday Trans.*, 86 (1990) 959. https://doi.org/10.1039/FT9908600959

123. L. Vayssieres., K. Keis., S. E. Lindquist., A. Hagfeldt, *J. Phys. Chem.* B, 105 (2001) 3350. https://doi.org/10.1021/jp010026s
124. Y. W. Heo, V. Varadarajan, M. Kaufman, K. Kim, D. P. Norton, F. Ren and P. H. Fleming, *Appl. Phys. Lett.* 81 (2002) 3046. https://doi.org/10.1063/1.1512829
125. W. T. Chiou, W. Y. Wu and J. M. Ting, *Diam. Relat. Mater.*, 12 (2003) 1841. https://doi.org/10.1016/S0925-9635(03)00274-7
126. Y. Sun, G. M. Fuge and M. N. R. Ashfold, *Chem. Phys. Lett.*, 396 (2004) 21. https://doi.org/10.1016/j.cplett.2004.07.110
127. J. I. Hong, J. Bae, Z. L. Wang and R. L. Snyder, *Nanotechnol.*, 20 (2009) 085609. https://doi.org/10.1088/0957-4484/20/8/085609
128. D. D. Lin, W. Pan and H. J. Wu, *Am. Ceram. Soc.*, 90 (2007) 71. https://doi.org/10.1111/j.1551-2916.2006.01366.x
129. D. Lin, H. Wu and W. Pan, *Adv. Mater*., 19 (2007) 3968. https://doi.org/10.1002/adma.200602802
130. X. M. Sui, C. L. Shao and Y. C. Liu, *Appl. Phys. Lett.*, 87 (2005) 113115. https://doi.org/10.1063/1.2048808
131. C. K. Xu, G. D. Xu, Y. K. Liu and G. H. Wang, *Solid State Commun.*, 122 (2002) 175. https://doi.org/10.1016/S0038-1098(02)00114-X
132. J. J. Wu, H. I. Wen, C. H. Tseng and S. C. Liu, *Adv. Funct. Mater.*, 14 (2004) 806. https://doi.org/10.1002/adfm.200305092
133. H. Zhang, D. R. Yang, X. Y. Ma, N. Du, J. B. Wu and D. L. Que, *J. Phys. Chem. B*, 110 (2006) 827. https://doi.org/10.1021/jp055351k
134. P. C. Chang and J. G. Lu, *IEEE Trans. Electron Dev.*, 55 (2008) 2977. https://doi.org/10.1109/TED.2008.2005181
135. S. Xu, Y. Wei, M. Kirkham, J. Liu, W. Mai, D. Davidovic, R. L. Snyder and Z. L. Wang, *J. Am. Chem. Soc.*, 130 (2008) 14958. https://doi.org/10.1021/ja806952j
136. T. Wang, Z. Jiao, T. Chen, Y. Li, W. Ren, S. Lin, G. Lu, J. Yec and Y. Bi, *Nanoscale*, 5 (2013) 7552. https://doi.org/10.1039/c3nr01459b
137. S. Xu, N. Adiga, S. Ba, T. Dasgupta, C. F. J. Wu and Z. L. Wang, *ACS Nano*, 3 (2009) 1803. https://doi.org/10.1021/nn900523p
138. M. H. Huang, Y. Wu, H. Feick, N. Tran, E. Weber and P. Yang, *Adv. Mater.*, 13 (2001) 113. https://doi.org/10.1002/1521-4095(200101)13:2<113::AID-ADMA113>3.0.CO;2-H
139. Y. C. Kong, D. P. Yu, B. Zhang, W. Fang and S. Q. Feng, *Appl. Phys. Lett.*, 78 (2001) 407. https://doi.org/10.1063/1.1342050
140. J. J. Wu and S.-C. Liu, *Adv. Mater.*, 14 (2002) 215. https://doi.org/10.1002/1521-4095(20020205)14:3<215::AID-ADMA215>3.0.CO;2-J
141. J. J. Wu and S.-C. Liu, *J. Phys. Chem. B.*, 106 (2002) 9546. https://doi.org/10.1021/jp025969j
142. J. Zhang, L. Sun, H. Pan, C. Liao and C. Yan, *New J. Chem.*, 26 (2002) 33. https://doi.org/10.1039/b108172a
143. Y. Li, G. W. Meng and L. D. Zhang, F. Phillipp, *Appl. Phys. Lett.*, 76 (2000) 2011. https://doi.org/10.1063/1.126238
144. L. Vayssieres, *Adv. Mater.*, 15 (2003) 464. https://doi.org/10.1002/adma.200390108
145. L. Vayssieres, K. Keis, A. Hagfeldt and S. Lindquist, *Chem. Mater.*, 13 (2001) 4395. https://doi.org/10.1021/cm011160s
146. L. E. Greene, M. Law, J. Goldberger, F. Kim, J. C. Johnson, Y. Zhang, R. J. Saykally and P. Yang, *Angew. Chem. Int. Ed.*, 42 (2003) 3031. https://doi.org/10.1002/anie.200351461
147. J. Choy, E. Jang, J. Won, J. Chung, D. Jang, and Y. Kim, *Adv. Mater.*, 15 (2003) 1911. https://doi.org/10.1002/adma.200305327
148. K. Govender, D. Boyle, P. Kenway and P. O'Brien, *J. Mater. Chem.*, 14 (2004) 2527. https://doi.org/10.1039/B404784B

149. K. Govender, D. S. Boyle, P. B. Kenway and P. J. O'Brien, *Mater. Chem.*, 14 (2004) 2575. https://doi.org/10.1039/B404784B
150. X. Wang, Q. Zhang, Q. Wan, G. Dai, C. Zhou and B. Zou, *J. Phys. Chem. C*, 115 (2011) 2769. https://doi.org/10.1021/jp1096822
151. X. Liu, W. Huang, H. Cheng, B. Huang, D. Bai, F. Fu, H. Wu, and L. Li, *Appl. Surf. Sci.*, 356 (2015) 240. https://doi.org/10.1016/j.apsusc.2015.08.075
152. A. Leelavathi, G. Madras and N. Ravishankar, *Phys. Chem. Chem. Phys.*, 15 (2013) 10795. https://doi.org/10.1039/c3cp51058a
153. X. Liu, L. Ye1, S. Liu, Y. Li and X. Ji, *Sci. Rep.*, 6 (2016). doi:10.1038/srep38474.
154. J. F. Zang, C. M. Li, X. Q. Cui, J. X. Wang, X. W. Sun, H. Dong and C. Q. Sun, *Electroanal.*, 19 (2007) 1008. https://doi.org/10.1002/elan.200603808
155. S. Baruah; Dutta, *J. Cryst. Growth*, 311 (2009) 2549. https://doi.org/10.1016/j.jcrysgro.2009.01.135
156. S. Xu, Y. Shen, Y. Ding and Z. L. Wang, *Adv. Funct. Mater.*, 20 (2010) 1493. https://doi.org/10.1002/adfm.201000230
157. C. Woll, *Prog. Surf. Sci.*, 82 (2007) 55. https://doi.org/10.1016/j.progsurf.2006.12.002
158. A. S. Kamble, B. B. Sinha, K. Chung, M. G. Gil, V. Burungale, C. J. Park, J. H. Kim and P. S. Patil, *Electrochim. Acta*, 149 (2014) 386. https://doi.org/10.1016/j.electacta.2014.10.049
159. W. J. Li, E. W. Shi, W. Z. Zhong and Z. W. Yin, *J. Cryst. Growth*, 203 (1999) 186. https://doi.org/10.1016/S0022-0248(99)00076-7
160. L. N. Demianets, D. V. Kostomarov, I. P. Kuzmina and S. V. Pushko, *Crystallogr. Rep.*, 47 (2002) S86. https://doi.org/10.1134/1.1529962
161. S. Yamabi and H. Imai, *J. Mater. Chem.*, 12 (2002) 3773. https://doi.org/10.1039/b205384e
162. A. Kawska, P. Duchstein, O. Hochrein and D. Zahn, *Nano Lett.*, 8 (2008) 2336. https://doi.org/10.1021/nl801169x
163. B. Liu and H. C. Zeng, *Langmuir*, 20 (2004) 4196. https://doi.org/10.1021/la035264o
164. R. Viswanatha, H. Amenitsch and D. D. Sarma, *J. Am. Chem. Soc.*, 129 (2007) 4470. https://doi.org/10.1021/ja068161b
165. L. N. Demianets and D. V. Kostomarov, *Ann. Chim. Sci. Mat.*, 26 (2001) 193. https://doi.org/10.1016/S0151-9107(01)90035-2
166. L. N. Demyanets, D. V. Kostomarov and I. P. Kuz-mina, *Inorg. Mater.*, 38 (2002) 124. https://doi.org/10.1023/A:1014008909633
167. B. Cheng and E. T. Samulski, *Chem. Commun.*, (2004) 986. https://doi.org/10.1039/b316435g
168. H. L. Cao, X. F. Qian, Q. Gong, W. M. Du, X. D. Ma and Z. K. Zhu, *Nanotechnol.*, 17 (2006) 3632. https://doi.org/10.1088/0957-4484/17/15/002
169. B. Liu and H. C. Zeng, *J. Am. Chem. Soc.*, 125 (2003) 4430. https://doi.org/10.1021/ja0299452
170. J. Zhang, L. D. Sun, J. L. Yin, H. L. Su, C. S. Liao and C. H. Yan, *Chem. Mater.*, 14 (2002) 4172. https://doi.org/10.1021/cm020077h
171. X. M. Hou, F. Zhou, Y. B. Sun and W. M. Liu, *Mater. Lett.*, 61 (2007) 1789. https://doi.org/10.1016/j.matlet.2006.07.133
172. T. Alammar and A. V. Mudring, *Mater. Lett.*, 63 (2009) 732. https://doi.org/10.1016/j.matlet.2008.12.035
173. T. Wang, B. Jin, Z. Jiao, G. Lu, J. Yeb and Y. Bi, *J. Mater. Chem. A*, 2 (2014) 15553. https://doi.org/10.1039/C4TA02960G
174. M. Yin, Y. Gu, I. L. Kuskovsky, T. Andelman, Y. Zhu, G. F. Neumark and S. O'Brien, *J. Am. Chem. Soc.*, 126 (2004) 6206. https://doi.org/10.1021/ja031696+
175. C. Pacholski, A. Kornowski and H. Weller, Angew. *Chem. Int. Edit.*, 41 (2002) 1188. https://doi.org/10.1002/1521-3773(20020402)41:7<1188::AID-ANIE1188>3.0.CO;2-5

176. D. F. Zhang, L. D. Sun, J. L. Yin, C. H. Yan and R. M. Wang, *J. Phys. Chem. B*, 109 (2005) 8786. https://doi.org/10.1021/jp050631l
177. L. Guo, Y. L. Ji, H. B. Xu, P. Simon and Z. Y. Wu, *J. Am. Chem. Soc.*, 124 (2002) 14864. https://doi.org/10.1021/ja027947g
178. J. P. Liu, X. T. Huang, Y. Y. Li, X. X. Ji, Z. K. Li, X. He and F. L. Sun, *J. Phys. Chem. C*, 111 (2007) 4990. https://doi.org/10.1021/jp067782o
179. Y. F. Gao, M. Nagai, T. C. Chang, J. Shyue and J. Cryst. *Growth Des.*, 7 (2007) 2467. https://doi.org/10.1021/cg060934k
180. Y. Tak and K. J. Yong, *J. Phys. Chem. B*, 109 (2005) 19263. https://doi.org/10.1021/jp0538767
181. C. K. Xu, P. Shin, L. L. Cao and D. Gao, *J. Phys. Chem., C.*, 114 (2010) 125. https://doi.org/10.1021/jp9085415
182. B. Postels, H. H. Wehmann, A. Bakin, M. Kreye, D. Fuhrmann, J. Blaesing, A. Hangleiter, A. Krost, and A. Waag, *Nanotechnol.*, 18 (2007) 195602. http://iopscience.iop.org/article/10.1088/0957-4484/18/19/195602/meta
183. G. M. Hua, Y. Zhang, J. X. Zhang, X. L. Cao, W. Xu and L. D. Zhang, *Mater. Lett.*, 62 (2008) 4109. https://doi.org/10.1016/j.matlet.2008.06.018
184. Q. Tang, W. J. Zhou, J. M. Shen, W. Zhang, L. F. Kong and Y. T. Qian, *Chem. Commun.*, (2004) 712. https://doi.org/10.1039/b313387g
185. D. S. Boyle, K. Govender and P. O'Brien, *Chem. Commun.*, (2002) 80. https://doi.org/10.1039/b110079n
186. L. Vayssieres, *Adv. Mater.*, 15 (2003) 464. https://doi.org/10.1002/adma.200390108
187. S. Xu and Z. L. Wang, *Nano Res.*, 4 (2011) 1013. https://doi.org/10.1007/s12274-011-0160-7
188. F. A. Kröger, The Chemistry of Imperfect Crystals. 2nd Edition, North Holland, Amsterdam, (1974) 73. https://doi.org/10.1002/crat.19740090719
189. G. D. Mahan, *J. Appl. Phys.*, 54 (1983) 3825. https://doi.org/10.1063/1.332607
190. T. K. Gupta, *J. Am. Ceram. Soc.*, 73 (1990) 1817. https://doi.org/10.1111/j.1151-2916.1990.tb05232.x
191. J. Han, P. Q. Mantas and A. M. R. Senos, *J. Eur. Ceram. Soc.*, 22 (2002) 49. https://doi.org/10.1016/S0955-2219(01)00241-2
192. K. I. Hagemark, *J. Solid State Chem.*, 16 (1976) 293. https://doi.org/10.1016/0022-4596(76)90044-X
193. D. G. Thomas, *J. Phys. Chem. Solids.*, 3 (1957) 229. https://doi.org/10.1016/0022-3697(57)90027-6
194. G. W. Tomlins, *J. Appl. Phys.*, 87 (2000) 117. https://doi.org/10.1063/1.371832
195. B. J. Wuensch and H. J. Tuller, *J. Phys. Chem. Solids.*, 55 (1994) 975. https://doi.org/10.1016/0022-3697(94)90117-1
196. W. D. Kingery, H. U. Bower and D. R. Uhlman, Introduction to Ceramics. 2nd Edition, John Wiley and Sons, New York, (1976). ISBN: 978-0-471-47860-7
197. K. I. Hagemark and L. C. Chacka, *J. Solid State Chem.*, 15 (1975) 261. https://doi.org/10.1016/0022-4596(75)90211-X
198. K. H. Tam, C. K. Cheung, Y. H. Leung, A. B. Djurisic, C. C. Ling, C. D. Beling, S. Fung, W. M. Kwok, W. K. Chan, D. L. Phillips, and W. K. Ding, *J. Phys. Chem. B* 110 (2006) 20865. https://doi.org/10.1021/jp063239w
199. S. B. A. Hamid, S. J. The and C. W. Lai, *Catalysts*, 7 (2017) 93. https://doi.org/10.3390/catal7030093
200. J. Chang and E. R. Waclawik, *Cryst. Eng. Comm.*, 14 (2012) 4041. https://doi.org/10.1039/c2ce25154j
201. E. S. Jang, J. H. Won, S. J. Hwang and J. H. Choy, *Adv. Mater.*, 18 (2006) 3309. https://doi.org/10.1002/adma.200601455
202. J. H. Zeng, B. B. Jin and Y. F. Wang, *Chem. Phys. Lett.*, 472 (2009) 90. https://doi.org/10.1016/j.cplett.2009.02.082

203. E. Debroye, J. V. Loon, H. Yuan, K. P. F. Janssen, Z. Lou, S. Kim, T. Majima and M. B. J. Roeffaers. *J. Phys. Chem. Lett.*, 8 (2017) 340. https://doi.org/10.1021/acs.jpclett.6b02577
204. R. Boppella, K. Anjaneyulu, P. Basak and S. V. Manorama. *J. Phys. Chem. C*, 117 (2013) 4597. https://doi.org/10.1021/jp311443s
205. E. S. Jang, J. H. Won, S. J. Hwang and J. H. Choy. *Adv. Mater.*, 18 (2006) 3309. https://doi.org/10.1002/adma.200601455
206. J. H. Zeng, B. B. Jin and Y. F. Wang, *Chem. Phys. Lett.*, 472 (2009) 90. https://doi.org/10.1016/j.cplett.2009.02.082
207. M. Huang, Y. Yan, W Feng, S. Weng, Z. Zheng, X. Fu and P. Liu, *Cryst. Growth Des.*, 14 (2014) 2179. https://doi.org/10.1021/cg401676r
208. A. McLaren; T. Li, G. Valdes-Solis and S. C. Tsang. *J. Am. Chem. Soc.*, 131 (2009) 12540. https://doi.org/10.1021/ja9052703
209. J. H. Choy, E. S. Jang, J. H. Won, J. H. Chung, D. J. Jang and Y. W. Kim, *Adv. Mater.*, 15 (2003) 1911. https://doi.org/10.1002/adma.20030532
210. E. S. Jang, J. H. Won, S. J. Hwang and J. H. Choy, *Adv. Mater.*, 18 (2006). https://doi.org/10.1002/adma.200601455
211. Z. R. Tian, J. A. Voigt, B. McKenzie, M. J. McDermott, *J. Am. Chem. Soc.*, 124 (2002) 12954. https://doi.org/10.1021/ja0279545
212. Z. R. Tian, J. A. Voigt, J. Liu, B. McKenzie, M. J. McDermott, M. A. Rodriguez, H. Konishi and H. Xu, *Nat. Mater.*, 2 (2003) 821. https://doi.org/10.1038/nmat1014
213. A. A. Beigi, S. Fatemi and Z. Salehi, *J. CO2 Util.* 7 (2014) 23. https://doi.org/10.1016/j.jcou.2014.06.003
214. M. Li, L. Zhang, X. Fan, Y. Zhou, M. Wu and J. Shi, *J. Mater. Chem., A* 3 (2015) 5189. https://doi.org/10.1039/C4TA06295G
215. Y. Bessekhouad, D. Robert and J. V. Weber, *J. Photochem. Photobiol. A*, 163 (2004) 569. https://doi.org/10.1016/j.jphotochem.2004.02.006
216. C. Wang, R. L. Thompson, P. Ohodnicki, J. Baltrus and C. Matranga, *J. Mater. Chem.*, 21 (2011) 13452. https://doi.org/10.1039/c1jm12367j
217. X. Li, H. Liu, D. Luo, J. Li, Y. Huang, H. Li, Y. Fang, Y. Xu and L. Zhu, *Chem. Eng. J.*, 180 (2012) 151. https://doi.org/10.1016/j.cej.2011.11.029
218. G. Zeng, J. Qiu, Z. Li, P. Pavaskar and S. B. Cronin, *ACS Catal.*, 4 (2014) 3512. https://doi.org/10.1021/cs500697w
219. C. Wang, R. L. Thompson, J. Baltrus and C. Matranga, *J. Phys. Chem. Lett.*, 1 (2010) 48. https://doi.org/10.1021/jz9000032
220. United Nations. The World Population Situation in (2014): A Concise Report. New York (2014). https://unwgfoodandhunger.files.wordpress.com/2015/09/concise-report-on-the-world-population-situation-in-2014.pdf
221. World Bank. Sustainable low-carbon city development in China. Axel Baeumler, Ede Ijjasz-Vasquez, and ShomikMehndiratta, eds. Washington, D.C, (2012). doi: 10.1596/978-0-8213-8987-4
222. Intergovernmental Panel on Climate Change (IPCC). Climate Change (2014): Impacts, Adaptation, and Vulnerability. Part A: Global and Sectoral Aspects. Contribution of Working Group II to the Fifth Assessment Report of the Intergovernmental Panel on Climate Change. Cambridge University Press, Cambridge, United Kingdom and New York, NY, USA, (2014) 1132. http://www.ipcc.ch/report/ar5/wg2/
223. World Bank. Sustainable low-carbon city development in China. Axel Baeumler, Ede Ijjasz-Vasquez, and ShomikMehndiratta, eds. Washington, D. C. Note: based on (2000) data (2012). doi: 10.1596/978-0-8213-8987-4
224. United Nations (UN). World Urbanization Prospects, (2014) Revision. Highlights. New York. http://esa.un.org/unpd/wup/.
225. K. Nina, D. Fridley, L. Hong. *Sust. Cities Soc.*, (2014) 110.
226. World Bank. World Bank Open Data (2015). http://data.worldbank.org/

227. International Energy Agency (IEA). (2007). World Energy Outlook (2007)-China and India Insights. IEA: Paris, France. https://www.iea.org/publications/freepublications/publication/weo_(2007).pdf
228. Fridley, D., Zheng, N., Qin, Y. (2011). Inventory of China's Energy-Related CO2 Emissions in (2008). Berkeley, CA: Lawrence Berkeley National Laboratory. https://china.lbl.gov/sites/all/files/lbl-4600e-(2008)-c02-inventorymarch-(2011).pdfhttps://doi.org/10.2172/1016716
229. L. Berkeley National Laboratory calculations based on the Reinventing Fire: China model, data from China's National Bureau of Statistics, and China-specific CO2 emissions factors. https://www.eceee.org/.../reinventing-fire-china...china8217s.../1-242-17_Price.pdf/
230. Y. Wang, Q. Song, J. He and Y. Qi. Climate *Policy*, 15 (2015) 581. https://doi.org/10.1080/14693062.2015.1050347
31. Carbon Disclosure Project (CDP). (2015). CDP Open Data Portal. https://data.cdp.net/Cities/Citywide-GHG-Emissions-(2013)/qznk-mn6r. Note that these emissions are in units of tCO2e
232. E. V. Kondratenko, G. Mul, J. Baltrusaitis. G. O. Larrazábal and J. Pérez-Ramirez, *Energ. Environm. Sci.,* 6 (2013) 3112. https://doi.org/10.1039/c3ee41272e
233. W. Wang, S. Wang, X. Ma and J. Gong. *Chem. Soc. Rev.*, 40 (2011) 3703. https://doi.org/10.1039/c1cs15008a
234. Z. Jianf, T. Xiao, V.L. Kuznetsov and P. P. Edwards, *Phil. Trans. R. Soc. A,* 368 (2010) 3343. https://doi.org/10.1098/rsta.2010.0119
235. G. Centi, E. A. Quadrelli and S. Perathoner. *Energ. Environ. Sci.*, 6 (2013) 1711. https://doi.org/10.1039/c3ee00056g
236. I. Ganesh, Renew. *Sust. Energ. Rev.*, 31 (2014) 221. https://doi.org/10.1016/j.rser.2013.11.045
237. C. Graves, S. D. Ebbesen, M. Mogensen and K. S. Lackner. *Renew. Sust. Energy Rev.*, 15 (2011) 1. https://doi.org/10.1016/j.rser.2010.07.014
238. W. H. Wang, Y. Himeda, J. T. Muckermann, G. F. Manbeck and E. Fujita. *Chem. Rev.*, 115 (2015) 12936. https://doi.org/10.1021/acs.chemrev.5b00197
239. Y. N. Li, R. Ma, L. N. He and Z. F. Diao. *Catal. Sci. Technol.*, 4 (2014) 1498. https://doi.org/10.1039/C3CY00564J
240. A. Goeppert, M. Czaun, J. P. Jones, G. K. Surya Prakash and G. A. Olah. *Chem. Soc. Rev.*, 43 (2014) 7995. https://doi.org/10.1039/C4CS00122B
241. M. Behrens et al. *Science*, 336 (2012) 893. https://doi.org/10.1126/science.1219831
242. S. C. Roy, O. K. Varghese, M. Paulose and C. A. Grimes. *ACS Nano*., 4 (2010) 1259. doi: 10.1021/nn9015423
243. M. S. Azmina, R. Md. Nor, H. A. Rafaie, N. S. A. Razak, S. F. A. Sani and Z. Osman, *Appl. Nanosci*, 7 (2017) 885. https://doi.org/10.1007/s13204-017-0626-3